EEG Signal Classification for Brain Computer Interface Applications

ECOLE POLYTECHNIQUE FEDERALE DE LAUSANNE

Jorge Baztarrica Ochoa

Responsible Assistant : **Gary Garcia Molina.**

Professor : **Touradj Ebrahimi**

March 28th, 2002

Abstract

Recent advances in computer hardware and signal processing have made possible the use of EEG signals or “brain waves” for communication between humans and computers. Locked-in patients have now a way to communicate with the outside world, but even with the last modern techniques, such systems still suffer communication rates on the order of 2-3 tasks/minute. In addition, existing systems are not likely to be designed with flexibility in mind, leading to slow systems that are difficult to improve.

This diploma project explores the effectiveness of Time – Frequency Analysis as a technique of classifying different mental tasks through the use of the electroencephalogram (EEG). EEG signals from several subjects through 6 channels (electrodes) have been studied during the performance of five mental tasks (a baseline resting task, mental multiplication, geometric figure rotation, mental letter composition, and counting). Improved off-line classification of two of them (“geometric figure rotation” and “mental letter composition”), for which poor results had been obtained with autoregressive models before, were the principal objective of this project.

Different methods based on Time Frequency Representations have been considered for the classification between the two tasks mentioned above. A non-iterative method based on the Ambiguity Function was finally selected. The results indicate that this method is able to extract in half-second, distinguishing features from the data, that could be classified as belonging to one of the two tasks with an average percentage accuracy which tends to zero. The same results were found when the method was exported for five tasks EEG signal classification.

The work presented here is a part of a larger project, whose goal is to classify EEG signals belonging to a varied set of mental activities in a real time Brain Computer Interface, in order to investigate the feasibility of using different mental tasks as a wide communication channel between people and computers.

Statement

Classification des signaux EEG

L'utilisation de signaux EEG en tant que vecteur de communication entre homme et machine constitue l'un des défis actuels de la recherche en théorie du signal. L'élément principal d'un tel système de communication, plus connu sous le nom de « interface cerveau-machine » est l'interprétation des signaux EEG par rapport à des paramètres caractéristiques de l'activité électrique du cerveau.

La classification dans le domaine temps-fréquence est d'un intérêt particulier puisqu'il est possible de trouver des représentations adaptées pour la classification. Ainsi, on décompose un signal dans une base temps-fréquence qui maximise la variation inter-classe et minimise la variation intra-classe.

En outre, on peut donner une interprétation physiologique de la décomposition temps-fréquence en termes de bandes de fréquence caractérisant l'activité électrique du cerveau pour une tâche particulière.

Ce projet vise à l'étude des représentations temps-fréquence pour les signaux EEG et à l'interprétation de celles-ci dans le cadre de l'activité électrique du cerveau.

Le travail demandé consiste en 4 étapes :

1- Familiarisation avec l'état de l'art dans le domaine de l'analyse temps-fréquence des signaux.
2- Familiarisation avec la physiologie du cerveau : zones d'activité, bandes de fréquence caractéristique de l'activité électrique du cerveau, modèle électrique des neurones, mesure des signaux EEG et l'interprétation physique de la mesure des signaux EEG.
3- Etude des noyaux temps-fréquence Gaussiens et des combinaisons de ces noyaux pour trouver celui qui maximise la séparation inter-classe tout en minimisant la séparation intra-classe.
4- Proposer une interprétation physiologique reliant la représentation temps-fréquence à la théorie étudiée au point 2.

Le développement d'algorithmes est réalisé sous la forme de toolbox MATLAB.

Travaux à rendre selon directives ci-jointes.

Prof. T. Ebrahimi

Assistant responsable : **Gary Garcia Molina.**

Références :

[1] Jonathan R. Wolpaw et al., “Brain-computer interface technology: A review of the first international meeting”, IEEE Transactions on rehabilitation engineering, vol. 8, no. 2, pp. 164-173, June 2000.
[2] A. Hyvärinen et al., «Independent component analysis : A tutorial », Helsinki university of technology, Laboratory of computer and information science, April 1999. http://www.cis.hut.fi/projects/ica/
[3] M. Davy, C. Doncarli, “Optimal Kernels of time-frequency representations for signal classification”.
[4] Time-frequency toolbox Matlab, CNRS (France) and Rice University (USA), 1995-1996.
[5] S. Mallat, “Wavelet tour of signal processing”, Academic press, 1999, ISBN 0-12-466606-X.

Index of Contents

List of Figures

List of Tables

1. Preliminary.

1.1. Motivation.

My cousin presents muscular dystrophy. Every day that passes, his interaction with the world becomes more and more difficult.

People who are paralyzed or have other severe movement disorders need alternative methods for communication and control. Currently available augmentative communication methods require some muscle control. Whether they use one muscle group to supply the function normally provided by another (e.g., use extraocular muscles to drive a speech synthesizer) or detour around interruptions in normal pathways (e.g., use shoulder muscles to control activation of hand and forearm muscles [1]), they all require a measure of voluntary muscle function. Thus, they may not be useful for those who are totally paralyzed (e.g., by amyotrophic lateral sclerosis (ALS) or brainstem stroke) or have other severe motor disabilities. These individuals need an alternative communication channel that does not depend on muscle control. They need a method to express their wishes that does not rely on the brain's normal output pathways of peripheral nerves and muscles.

1.2. Objectives.

The use of EEG signals as a vector of communication between men and machines represents one of the current challenges in signal theory research. The principal element of such a communication system, more known as "Brain Computer Interface", is the interpretation of the EEG signals related to the characteristic parameters of brain electrical activity.

The role of signal processing is crucial in the development of a real-time Brain Computer Interface. Until recently, several improvements have been made in this area, but none of them have been successful enough to use them in a real system. The goal of creating more effective classification algorithms, have focused numerous investigations in the search of new techniques of feature extraction.

The main objective of this project is the establishment of a Time – Frequency method, which allows EEG signal classification between two given tasks ("geometric figure rotation" and "mental letter composing"), as well as the familiarization with the state of the art in time-frequency and Brain Computer Interface. The extension of this method to a five-task classification problem will be also considered.

2. Principles of electroencephalography.

2.1. The Nature of the EEG signals.

The electrical nature of the human nervous system has been recognized for more than a century. It is well known that the variation of the surface potential distribution on the scalp reflects functional activities emerging from the underlying brain [2.1]. This surface potential variation can be recorded by affixing an array of electrodes to the scalp, and measuring the voltage between pairs of these electrodes, which are then filtered, amplified, and recorded. The resulting data is called the EEG. Fig. 1-1 shows waveforms of a 10 second EEG segment containing six recording channels, while the recording sites are illustrated in Fig. 2-2. In our experiments, we have used the10-20 System of Electrode Placement, which is based on the relationship between the location of an electrode and the underlying area of cerebral cortex (the "10" and "20" refer to the 10% or 20% interelectrode distance) [2.7].

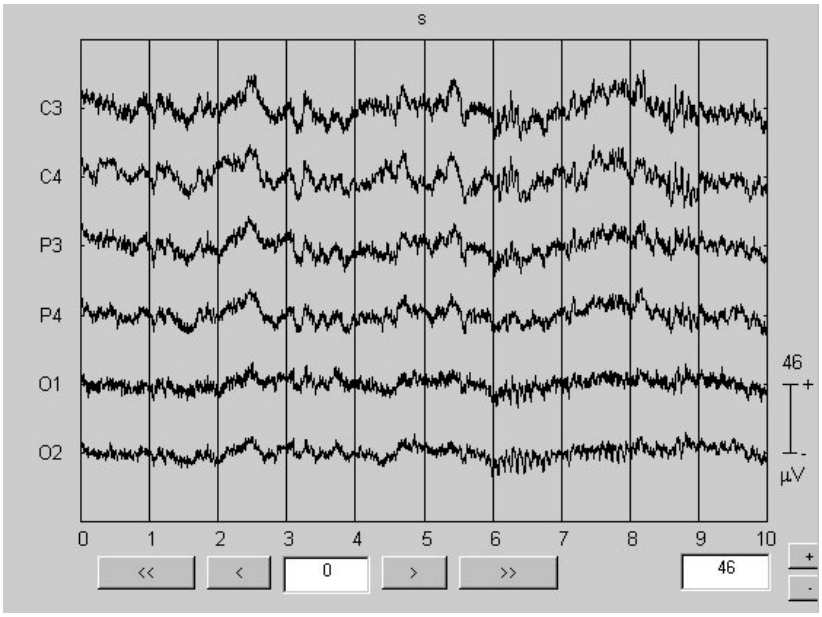

Figure 2-1. A segment of a multichannel EEG of an adult subject during a multiplication task.

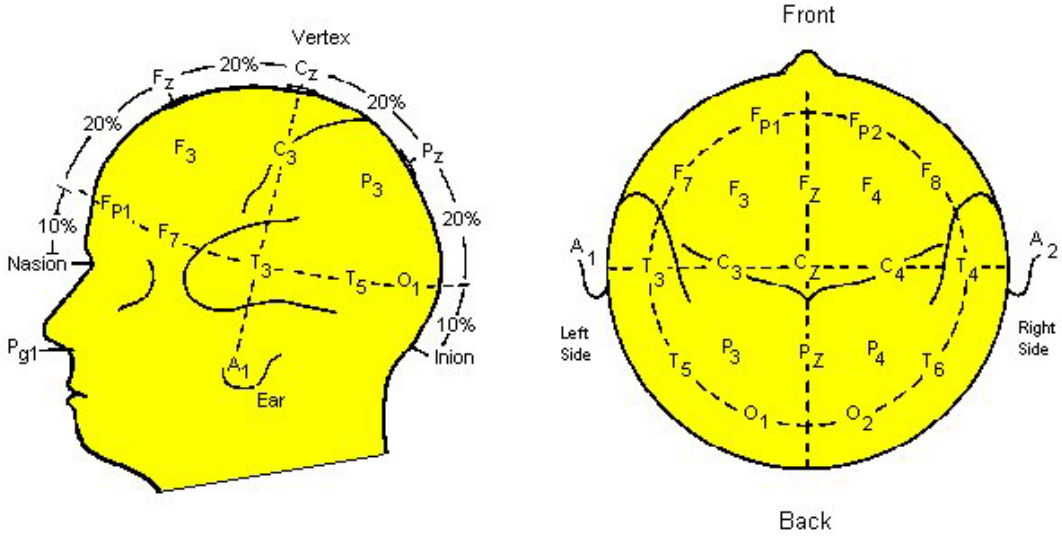

Figure 2-2. The 10-20 System of Electrode Placement.
Each site has a letter (to identify the lobe) and a number or another letter to identify the hemisphere location. The letters F, T, C, P, and O stand for Frontal, Temporal, Central, Parietal and Occipital. (Note that there is no "central lobe", but this is just used for identification purposes.) Even numbers (2,4,6,8) refer to the right hemisphere and odd numbers (1,3,5,7) refer to the left hemisphere. The z refers to an electrode placed on the midline.
Nasion: point between the forehead and nose.
Inion: Bump at back of skull

The EEG is thought to be the synchronized subthreshold dentritic potentials produced by the synaptic activity of many neurons summed [2.2]. In its formation not all types of brain activity have identical impact. The depth, orientation and intrinsic symmetry of connections in the cortex are significant in it. As it is exposed in previous works [2.2][2.3], pyramidal cells are thought to cause the strongest part of the EEG signal[1].

Nowadays, modern techniques for EEG acquisition collect these underlying electrical patterns from the scalp, and digitalize them for computer storage. Electrodes conduct voltage potentials as microvolt level signals, and carry them into amplifiers that magnify the signals approximately ten thousand times. The use of this technology depends strongly on the electrodes positioning and the electrodes contact. For this reason, electrodes are usually constructed from conductive materials, such us gold or silver chloride, with an approximative diameter of 1 cm, and subjects must also use a conductive gel on the scalp to maintain an acceptable signal to noise ratio. This method of EEG signal recording is shown in Fig. 2-3.

[1] For biological considerations about neurons structure, neurons type and its implication in EEG signals see annex 1.

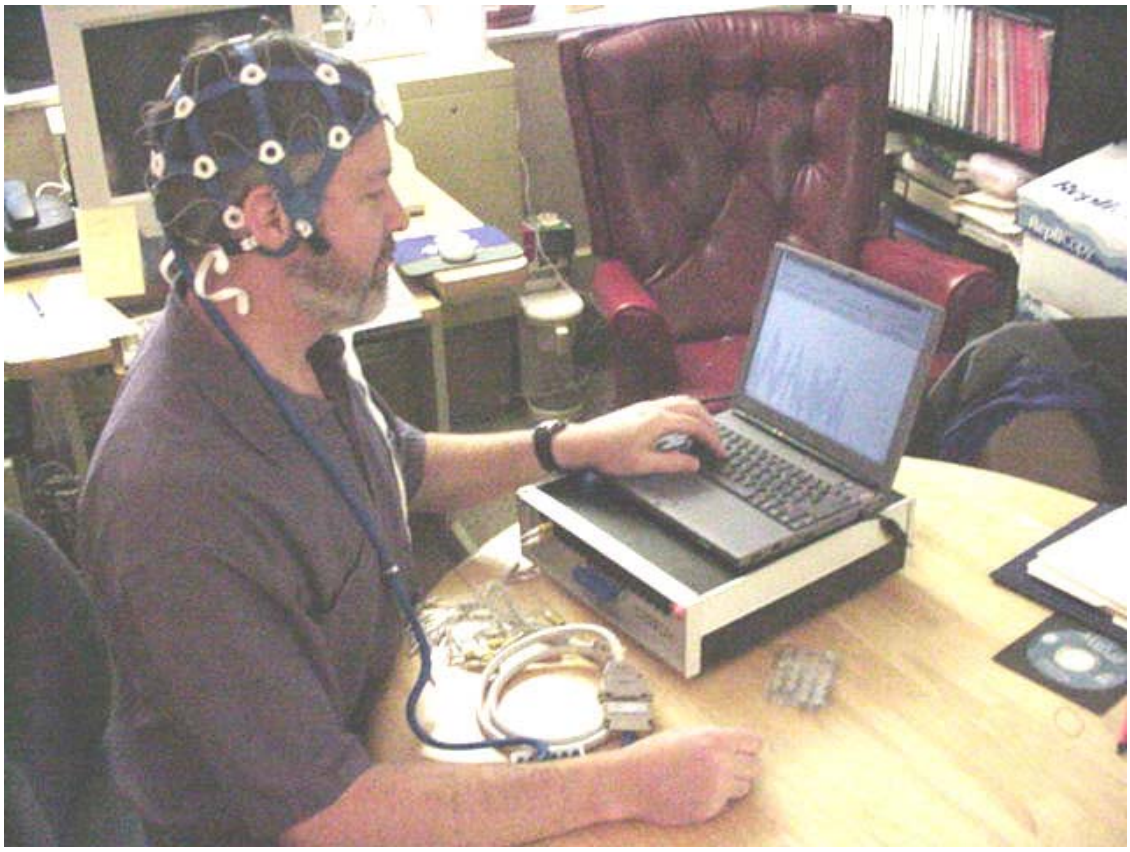

Figure 2-3. EEG signal recording.

2.2. EEG wave groups.

The analysis of continuous EEG signals or brain waves is complex, due to the large amount of information received from every electrode. As a science in itself, it has to be completed with its own set of perplexing nomenclature. Different waves, like so many radio stations, are categorized by the frequency of their emanations and, in some cases, by the shape of their waveforms. Although none of these waves is ever emitted alone, the state of consciousness of the individuals may make one frequency range more pronounced than others. Five types are particularly important:

BETA. The rate of change lies between 13 and 30 Hz, and usually has a low voltage between 5-30 μV (Fig. 2-6). *Beta* is the brain wave usually associated with active thinking, active attention, focus on the outside world or solving concrete problems. It can reach frequencies near 50 hertz during intense mental activity.

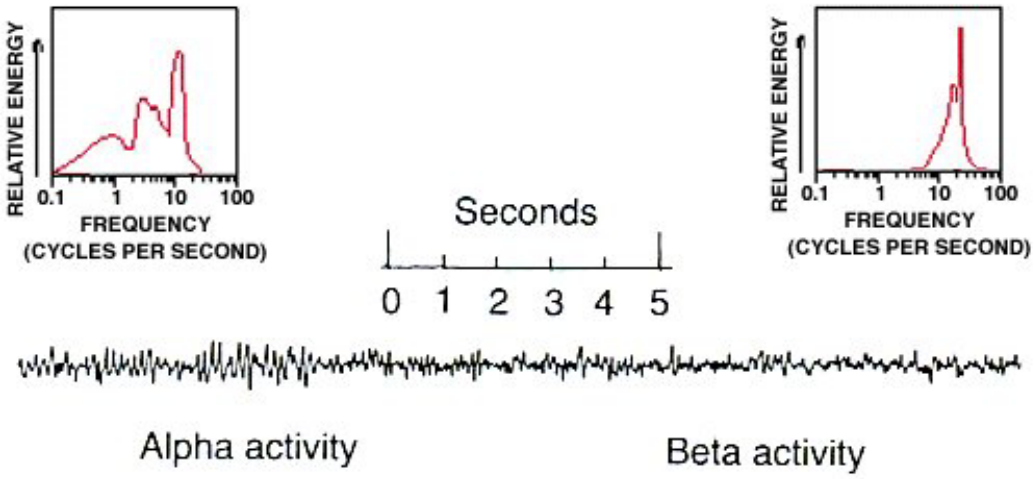

Figure 2-4. Alpha (left) and Beta (right) waves.

ALPHA. The rate of change lies between 8 and 13 Hz, with 30-50 μV amplitude (Fig 2-4). *Alpha* waves have been thought to indicate both a relaxed awareness and also inattention. They are strongest over the occipital (back of the head) cortex and also over frontal cortex. *Alpha* is the most prominent wave in the whole realm of brain activity and possibly covers a greater range than has been previously thought of. It is frequent to see a peak in the beta range as high as 20 Hz, which has the characteristics of an alpha state rather than a beta, and the setting in which such a response appears also leads to the same conclusion. *Alpha* alone seems to indicate an empty mind rather than a relaxed one, a mindless state rather than a passive one, and can be reduced or eliminated by opening the eyes, by hearing unfamiliar sounds, or by anxiety or mental concentration.

THETA. *Theta* waves lie within the range of 4 to 7 Hz, with an amplitude usually greater than 20 μ V. *Theta* arises from emotional stress, especially frustration or disappointment. *Theta* has been also associated with access to unconscious material, creative inspiration and deep meditation. The large dominant peak of the theta waves is around 7 Hz.

Figure 2-5. Theta wave.

DELTA. *Delta* waves lie within the range of 0.5 to 4 Hz, with variable amplitude. *Delta* waves are primarily associated with deep sleep, and in the waking state, were thought to

indicate physical defects in the brain. It is very easy to confuse artifact signals caused by the large muscles of the neck and jaw with the genuine delta responses. This is because the muscles are near the surface of the skin and produce large signals whereas the signal which is of interest originates deep in the brain and is severely attenuated in passing through the skull. Nevertheless, with an instant analysis EEG, it is easy to see when the response is caused by excessive movement.

Figure 2-6. Delta wave.

GAMMA. *Gamma* waves lie within the range of 35Hz and up. It is thought that this band reflects the mechanism of consciousness - the binding together of distinct modular brain functions into coherent percepts capable of behaving in a re-entrant fashion (feeding back on themselves over time to create a sense of stream-of-consciousness).

MU. It is an 8-12 Hz spontaneous EEG wave associated with motor activities and maximally recorded over motor cortex (Fig. 2-8). They diminish with movement or the intention to move. *Mu* wave is in the same frequency band as in the *alpha* wave (Fig. 2-7), but this last one is recorded over occipital cortex.

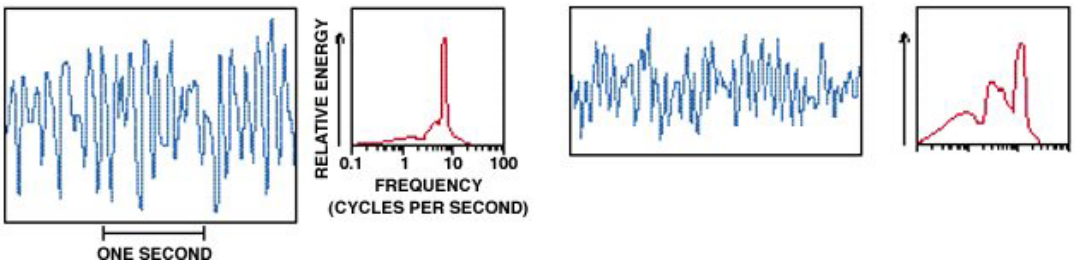

Figure 2-7. Mu (left) and alpha (right) waves.

Most attempts to control a computer with continuous EEG measurements work by monitoring *alpha* or *mu* waves, because people can learn to change the amplitude of these two waves by making the appropriate mental effort. A person might accomplish this result, for instance, by recalling some strongly stimulating image or by raising his or her level of attention.

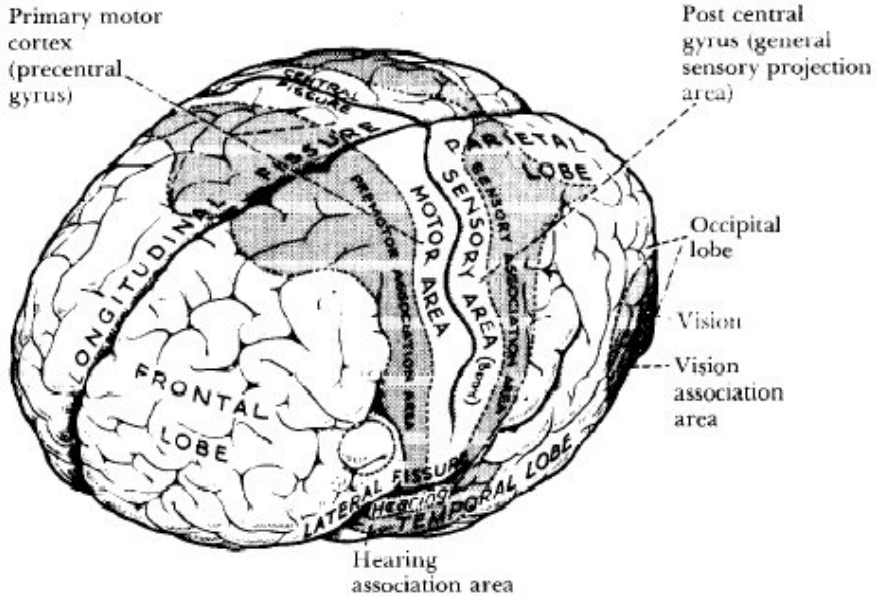

Figure 2-8. Cerebral hemispheres showing the motor areas (towards the front) and the sensory areas (towards the back).

3. Brain Computer Interface Technology.

3.1. System Overview.

A Brain-Computer Interface (BCI) is a system that acquires and analyzes neural signals with the goal of creating a communication channel directly between the brain and the computer. Such a channel potentially has multiple uses. For example:

- *Bioengineering applications*: assist devices for disabled people.
- *Human subject monitoring*: sleep disorders, neurological diseases, attention monitoring, and/or overall "mental state".
- *Neuroscience research*: real-time methods for correlating observable behavior with recorded neural signals.
- *Man – Machine Interaction*: Interface devices between human and computers, machines, …

For many years, people have speculated that electroencephalographic (EEG) activity or other measures of brain function might provide this new channel. Over the past decade, productive BCI research programs have begun. Facilitated and encouraged by the new understanding of brain functions and by the low-cost computer equipments, these programs have concentrated mainly in developing new communication and control technologies for people with severe neuromuscular disorders. The immediate goal is to provide communication capabilities so that any subject can control the external world without using the brain's normal output pathways of peripheral nerves and muscles.

Nowadays, such activities drive their efforts in:

- *Brain (neural) signal acquisition*: development of both invasive and non-invasive techniques for high quality signal acquisition.
- *Algorithms and processing*: advanced machine learning and signal processing algorithms, which take advantage of cheap/fast computing power (i.e. Moore's Law[2]) to enable online real-time processing.
- *Underlying neuroscience*: a better understanding of the neural code, the functional neuro-anatomy, the physiology and how these are related to perception and cognition, enabling signals to be interpreted in the context of the neurobiology.

[2] The observation that the power processing of integrated circuits has roughly doubled every year in the past decades and will continue doing the same in the next two decades.

Present BCI's use EEG activity recorded at the scalp to control cursor movement, select letters or icons, or operate a neuroprosthesis. The central element in each BCI is a translation algorithm that converts electrophysiological input from the user into output that controls external devices. BCI operation depends on effective interaction between two adaptive controllers: the user who encodes his or her commands in the electrophysiological input provided to the BCI, and the computer which recognizes the command contained in the input and expresses them in the device control.

Current BCI's have maximum information transfer rates of 5-25 bits/min. Achievement of greater speed and accuracy depends on improvements in:

- *Signal acquisition:* methods for increasing signal-to-noise ratio (SNR), signal-to-interference ratio (S/I)) as well as optimally combining spatial and temporal information.
- *Single trial analysis*: overcoming noise and interference in order to avoid averaging and maximize bit rate.
- *Co-learning*: jointly optimizing combined man-machine system and taking advantage of feedback.
- *Experimental paradigms for interpretable readable signals*: mapping the task to the brain state of the user (or vice versa).
- *Understanding algorithms and models within the context of the neurobiology*: building predictive models having neurophysiologically meaningful parameters and incorporating physically and biologically meaningful priors.

The common structure of a Brain Computer Interface is the following (Fig 3-1):

1) *Signal Acquisition*: the EEG signals are obtained from the brain through invasive or non-invasive methods (for example, electrodes). After, the signal is amplified and sampled.

2) Signal *Pre-Processing*: once the signals are acquired, it is necessary to clean them.

3) *Signal Classification*: once the signals are cleaned, they will be processed and classified to find out which kind of mental task the subject is performing.

4) *Computer Interaction*: once the signals are classified, they will be used by an appropriate algorithm for the development of a certain application.

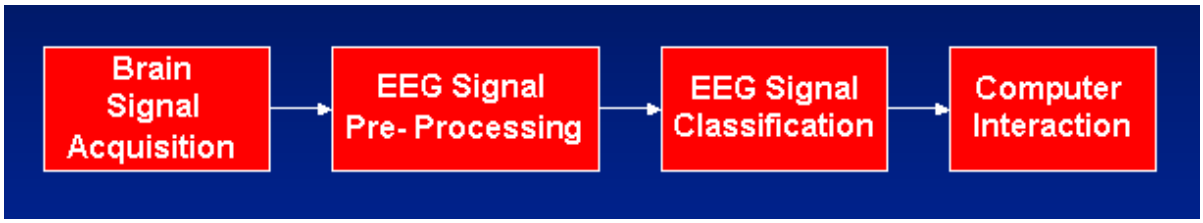

Figure 3-1. BCI common structure.

3.2. Neuropsychological signals used in BCI applications.

Interfaces based on brain signals require on-line detection of mental states from spontaneous activity: different cortical areas are activated while thinking different things (i.e. a mathematical computation, an imagined arm movement, a music composition, etc...). The information of these "mental states" can be recorded with different methods.

Neuropsychological signals can be generated by one or more of the following three: *implanted methods, evoked potentials (also known as event related potentials), and operant conditioning.* Both evoked potential and operant conditioning methods are normally externally-based BCIs as the electrodes are located on the scalp. Table 3.1 describes the different signals in common use. It may be noted that some of the described signals fit into multiple categories. As an example, single neural recordings may use operant conditioning in order to train neurons for control or may accept the natural occurring signals for control. Where this occurs, the signal is described under the category that best distinguishes it.

Implanted methods use signals from single or small groups of neurons in order to control a BCI. In most cases, the most suitable option for placing the electrodes is the motor cortex region, because of its direct relevance to motor tasks, its relative accessibility compared to motor areas deeper in the brain, and the relative ease of recording from its large pyramidal cells. These methods have the benefit of a much higher signal-to-noise ratio at the cost of being invasive. They require no remaining motor control and may provide either discrete or continuous control. While most systems are still in the experimental stage, Kennedy's group has forged ahead to provide control for locked-in patient JR [3.6] [3.7]. Kennedy's approach involves encouraging the growth of neural tissue into the hollow tip of a two-wire electrode known as a neurotrophic electrode. The tip contains growth factors that spur brain tissue to grow through it. Through an amplifier and antennas positioned between the skull and the scalp, the neural signals are transmitted to a computer, which can then use the signals to drive a mouse cursor. This technique has provided stable long term recording and patient JR has learned to produce synthetic speech with the BCI over a period of more than 426 days. It is unknown how well this technique would work on multiple individuals, but it has worked on both patients (JR and MH) who have been implanted.

Evoked potentials (EPs) are brain potentials that are evoked by the occurrence of a sensory stimulus. They are usually obtained by averaging a number of brief EEG segments time-registered to a stimulus in a simple task. In a BCI, EPs may provide control when the BCI application produces the appropriate stimuli. This paradigm has the benefit of requiring little to no training to use the BCI at the cost of having to make users wait for the relevant stimulus presentation. EPs offer discrete control for almost all users, as EPs are an inherent response.

Exogenous components, or those components influenced primarily by physical stimulus properties, generally take place within the first 200 milliseconds after stimulus onset. These components include a Negative waveform around 100 ms (N1) and a Positive waveform around 200 ms after stimulus onset (P2). **Visual evoked potentials** (VEPs) fall into this category. Sutter uses short visual stimuli in order to determine what command an individual is looking at and therefore wants to pick [3.8]. He also shows that implanting electrodes improves performance of an externally-based BCI. In a different approach, McMillan and colleagues have trained volunteers to control the amplitude of their steady-state VEPs to florescent tubes flashing at 13.25 Hz [3.9][3.10][3.11]. Using VEPs has the benefit of a quicker response than longer latency components. The VEP requires subject to have good visual control in order to look at the appropriate stimulus and allows for discrete control. As the VEP is an exogenous component, it should be relatively stable over time. Endogenous components, or those components influenced by cognitive factors, take place following the exogenous components. Around 1964, Chapman and Bragdon [3.12] as well as Sutton *et al*. [3.13] independently discovered a wave peaking at around 300 ms after task-relevant stimuli. This component is known as the P3 and is shown in Fig 3-2. While the P3 is evoked by many types of paradigms, the most common factors that influence it are stimulus frequency (less frequent stimuli produce a larger response) and task relevance. The P3 has been shown to be fairly stable in locked-in patients, re-appearing even after severe brain stem injuries [3.14]. Farwell and Donchin (University of Illinois) first showed that this signal may be successfully used in a BCI [3.15]. Using a broad cognitive signal like the P3 has the benefit of enabling control through a variety of modalities, as the P3 enables discrete control in response to both auditory and visual stimuli. As it is a cognitive component, the P3 has been known to change in response to subject's fatigue. In one study, a reduction in the P3 was attributed to fatigue after subjects performed the task for several hours [3.16].

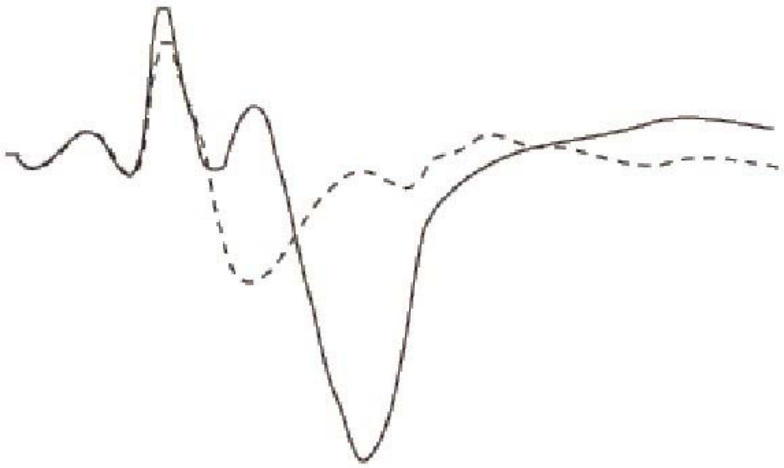

Figure 3-2. P3 evoked potential.
Solid line: the general form of the P3 component of the evoked potential (EP). The P3 is a cognitive EP that appears approximately 300 ms after a task relevant stimulus. In this image is represented by the biggest negative peak.
Dotted line: the general form of a non-task related response.

Operant conditioning is a method for modifying the behavior (an operant), which utilizes contingencies between a discriminative stimulus, an operant response, and a reinforcer to change the probability of a response occurring again in a given situation. In the BCI framework, it is used to train the patients to control their EEG. As it is presented in Table 3.1, several methods use **operant conditioning** on spontaneous EEG signals for BCI control. The main feature of this kind of signals is that it enables continuous rather than discrete control. This feature may also serve as a drawback: continuous control is fatiguing for subjects and fatigue may cause changes in performance since control is learned.

Signal name	Description
Mu and Alpha Wave Operant Conditioning [3.1] [3.24]	The *mu* wave is a 8-12 Hz spontaneous EEG wave associated with motor activities and maximally recorded over sensorimotor cortex. The *alpha* wave is in the same frequency band, but is recorded over occipital cortex. The amplitudes of these waves may be altered through biofeedback training.
Event-Related Synchronization /Desynchronization (ERS/ERD) Operant Conditioning [3.2][3.20][3.21][3.22][3.23]	Movement-related increases and decreases in specific frequency bands maximally located over brain's motor cortex. Individuals may be trained through biofeedback to alter the amplitude of signals in the appropriate frequency bands. These signals exist even when the individual imagines moving as the movement-related signals are preparatory rather than actual.
Slow Cortical Potential Operant Conditioning [3.4]	Large negative or positive shifts in the EEG signal lasting from 300ms up to several minutes. Individuals may be trained through biofeedback to produce these shifts.
P3 Component of the Evoked Potential [3.15]	A positive shift in the EEG signal approximately 300-400ms after a task relevant stimulus. Maximally located over the central parietal region, this is an inherent response and no training is necessary.
Short-Latency Visual Evoked Potentials [3.8]	To produce the component, a response to the presentation of a short visual stimulus is necessary. Maximally located over the occipital region, this is an inherent response and no training is necessary.
Individual Neuron Recordings [3.7][3.25]	Individuals receive implanted electrodes that may obtain responses from local neurons or even encourage neural tissue to grow into the implant. Operant conditioning may be used to achieve control or the natural response of a cell or cells may be used.
Steady-State Visual Evoked Potential (SSVER) [3.9][3.10][3.11]	A response to a visual stimulus modulated at a specific frequency. The SSVER is characterized by an increase in EEG activity at the stimulus frequency. Typically, the visual stimulus is generated using white fluorescent tubes modulated at around 13.25 Hz or by another kind of strobe light. A system may be constructed by conditioning individuals to modulate the amplitude of their response or by using multiple SSVERs for different system decisions.

Table 3.1. Common neuropsychological signals used in BCIs

Wolpaw and his colleagues train individuals to control their *mu* wave amplitude (Table 3.2) for cursor control [3.1]. *Mu* wave control does not require subjects to have any remaining motor control. For the cursor control task, normal subjects are trained on the order of 10-15 sessions to learn to move the cursor up/down. In the several papers examined, it appears that not all subjects obtain control, although most seem to during this time frame.

In related work, the Graz brain-computer interface trains people to control the amplitude of their ERS/ERD patterns. Subjects are trained over a few sessions in order to learn a cursor control task. As in the *mu* wave control, not all subjects learn to control the cursor accurately. Obtaining two out of six subjects who are not able to perform the cursor control task has been reported [3.2]. Part of the charm of this system is that it gives biofeedback to the user in the form of a moving cursor after training.

Slow cortical potentials serve as the signal in the Thought Translation Device, a communication device created by Biurbaumer's group in Germany [3.4].

While the signals discussed are used currently, other signals may be possible.

Several papers have been written on recognizing EEG signal differences during different mental calculations. These papers suggest that different parts of the brain are active during different types of mental calculation, and if these different tasks may be accurately recognized, they could be used in a BCI. Lin *et al.* [3.5] describe a study where five tasks were compared: multiplication problem solving, geometric figure rotation, mental letter composing, visual counting, and a baseline task where the subject was instructed to think about nothing in particular. Results from this experiment suggest that the easiest tasks to identify are multiplication problem solving and geometric figure rotation, but even these tasks are not easily identified. Other papers have concentrated on mental tasks, but none have found easily recognizable differences between different tasks [3.17][3.18].

3.3. BCI research: existing systems.

Different research groups work on communication channels between the brain and the computer. The leading groups are presented in alphabetical order in Table 3. 2. These experimental interfaces include the hardware used in the BCI, the underlying BCI backend software, and the user application. In assessing current systems, several factors must be considered, including five mentioned by Ben Schneiderman [3.19]:

1. What is the time to learn the system?
2. What is the speed of performance?
3. How many and what kinds of errors do users make?
4. How well do users maintain their knowledge after an hour, a day, or a week? What is their retention?

5. How much did users like using various aspects of the system? What is their subjective satisfaction?

System	Training Time	Number of choices	Speed	Errors	Retention	Subjective Satisfaction
Brain Response Interface [3.8]	10-60 min	64	30	10%	Excellent	Considered
SSVEP training [3.9][3.10][3.11]	6 hrs	N/A	Not	<20%	Not mentioned	Not discussed
P3 Character Recognition [3.15]	Minutes	36	4	5%	Excellent	Not discussed
Mu Wave training [3.1] [3.24]	15-20 sessions	2	20	10%	Not mentioned	Not discussed.
ERS/ERD [3.2][3.20][3.21] [3.22][3.23]	2-2.5 hrs.	2	Not available	<11%	Not mentioned	Not discussed
Thought Translation Device [3.4]	Months	27	2	10-30%	Not Good	Indirectly Disgusted
Implanted Device [3.7][3.25]	Months	N/A	2	Not reported	Excellent	Considered
Flexible Brain Computer Interface [3.26]	Not mentioned	2	3	15%	Not mentioned	Not discussed

Table 3. 2. Comparison between existing BCIs. The Speed is presented in average number of items or movements per minute.

1) The Brain Response Interface (Smith-Kettlewell Institute of Visual Sciences in San Francisco).

Sutter's Brain Response Interface (BRI) [3.8] uses visually evoked potentials (VEP's) produced in response to brief visual stimuli. These EP's are then used to give a discrete command to pick a certain part of a computer screen. Word processing output approaches 10-12 words/min. and accuracy approaches 90% with the use of epidural electrodes. This is the only system mentioned that uses implanted electrodes to obtain a stronger, less contaminated signal.

A BRI user watches a computer screen with a grid of 64 symbols (some of which lead to other pages of symbols) and concentrates a given symbol. A specific subgroup of these symbols undergoes a equiluminant red/green fine check or plain color pattern alteration in a simultaneous stimulator scheme at the monitor vertical refresh rate (40-70 frames/s). Sutter considered the usability of the system over time and since color alteration between red and green was almost as effective as having the monitor flicker, he chose to use the color alteration because it was shown to be much less fatiguing for users.

This system is basically the EEG version of an eye movement recognition system and contains similar problems because it assumes that the subject is always looking at a command on the computer screen.

2) P3 Character Recognition (University of Illinois, USA).

In a related approach, Farwell and Donchin use the P3 evoked potential [3.15]. A 6x6 grid containing letters from the alphabet is displayed on the computer monitor and users are asked to select the letters in a word by counting the number of times that a row or column containing the letter flashes. Flashes occur at about 10 Hz and the desired letter flashes twice in every set of twelve flashes. The average response to each row and column is computed and the P3 amplitude is measured. Response amplitude is reliably larger for the row and column containing the desired letter. After two training sessions, users are able to communicate at a rate of 2.3 characters/min, with accuracy rates of 95%. This system is currently only used in a research setting.

A positive aspect of using a longer latency component such as the P3 is that it enables differentiating between when the user is looking at the computer screen or looking someplace else (as the P3 only occurs in certain stimulus conditions). Unfortunately, this system is also slow, because of the need to wait for the appropriate stimulus presentation and because the stimuli are averaged over trials, and can cause epilepsy in some subjects.

3) ERS/ERD Cursor Control (University of Technology Graz, Austria)

Pfurtscheller and his colleagues take a different approach [3.22] [3.20] [3.2] [3.21][3.23]. Using multiple electrodes placed over sensorimotor cortex they monitor event-related synchronization/ desynchronization (ERS/ERD) [64]. In all sessions, epochs with eye and muscle artifact are automatically rejected. This rejection can slow down subject performance. As this is a research system, the user application is a simple screen that allows control of a cursor in either the left or right direction. In another experiment, for a single trial the screen first appears blank, then a target box is shown on one side of the screen. A cross hair appears to let the user know that he/she must begin trying to move the cursor towards the box. Feedback may be Delayed or immediate and different experiments have slightly different displays and protocols. After two training

sessions, three out of five student subjects were able to move a cursor right or left with accuracy rates from 89-100%. Unfortunately, the other two students performed at 60% and 51%. When a third category was added for classification, performance dropped to a low of 60% in the best case [3.23].

4) A Steady State Visual Evoked Potential BCI (Wright-Patterson Air Force Base, The Air Force Research Laboratory, USA).

Middendorf and colleagues use operant conditioning methods in order to train volunteers to control the amplitude of the steady-state visual evoked potential (SSVEP) to florescent tubes flashing at 13.25 Hz [3.11][3.10][3.9]. This method of control may be considered as continuous as the amplitude may change in a continuous fashion. Either a horizontal light bar or audio feedback is provided when electrodes located over the occipital cortex measure changes in signal amplitude. If the VEP amplitude is below or above a specified threshold for a specific time period, discrete control outputs are generated. After around 6 hours of training, users may have an accuracy rate of greater than 80% in commanding a flight simulator to roll left or right.

Recognizing that the SSVEP may also be used as a natural response, Middendorf and his colleagues have recently concentrated on experiments involving the natural SSVEP. When the SSVEP is used as a natural response, virtually no training is needed in order to use the system. The experimental task for testing this method of control has been to have subjects select virtual buttons on a computer screen. From the 8 subjects participating in the experiment, the average percent correct was 92% with an average selection time of 2.1 seconds.

5) Mu Wave Cursor Control (Wadsworth Center, Albany, USA).

Wolpaw and his colleagues free their subjects from being tied to a flashing florescent tube by training subjects to modify their *mu* wave [3.24][3.1]. This method of control is continuous as the *mu* wave may be altered in a continuous manner. It can be attenuated by movement and tactile stimulation as well as by imagined movement. A subject's main task is to move a cursor up or down on a computer screen. While not all subjects are able to learn this type of biofeedback control, the subjects that do, perform with accuracy greater than or equal to 90%. These experiments have also been extended to two-dimensional cursor movement, but the accuracy of this is reported as having “not reached this level of accuracy” when compared to the one-dimensional control [3.11].

6) The Thought Translation Device (University of Tübingen, Germany)

As another application used with severely handicapped individuals, the Thought Translation Device, was developed by Birbaumer's lab [3.4]. Out of six patients with

ALS[3], 3 were able to use the Thought Translation Device. Of the other three, one lost motivation and later died and another used discontinuously the Thought Translation Device and was unable to regain control later.

The training program may use either auditory or visual feedback. The slow cortical potential is extracted from the regular EEG on-line, filtered, corrected for eye movement artifacts, and fed back to the patient. When using visual feedback, the target positivity/negativity is represented by a high and low box on the screen. A ball-shaped light moves toward or away from the target box depending on subject's performance. The subject is reinforced for good performance with the appearance of a happy face or a melodic sound sequence.

When a subject performs at least 75% correct, he/she is switched to the language support program. At level one, the alphabet is split into two halves (letter-banks) which are presented successively at the bottom of the screen for several seconds. If the subject selects the letter-bank being shown by generating a slow cortical potential shift, that side of the alphabet is split into two halves and so on, until a single letter is chosen.

7) An Implanted BCI (Georgia State University, USA).

The implanted brain-computer interface system devised by Kennedy and colleagues has been implanted into two patients [3.25][3.7]. These patients are trained to control a cursor with their implant and the velocity of the cursor is determined by the rate of neural firing. The neural waveshapes are converted to pulses and three pulses are an input to the computer mouse. The first and second pulses control X and Y position of the cursor and a third pulse as a mouse click or enter signal.

The patients are trained using software that contains a row of icons representing common phrases (Talk Assist developed at Georgia Tech). There are two paradigms using this software program and a third one using the visual keyboard. In the first paradigm, the cursor moves across the screen using one group of neural signals and down the screen using another group of larger amplitude signals. Starting in the top left corner, the patient enters the leftmost icon. He remains over the icon for two seconds so that the speech synthesizer is activated and phrases are produced. In the second paradigm, the patient is expected to move the cursor across the screen from one icon to the other. The patient is encouraged to be as accurate as possible, and then to speed up the cursor movement while attempting to remain accurate. In the third paradigm, a visual keyboard is shown and the patient is encouraged to spell his name as accurately and quickly as possible and then to spell anything else he wishes. Unfortunately, the maximum communication rate with this BCI has been around 3 characters per minute.

[3] ALS (Amyotrophic Lateral Sclerosis) is a fatal neuromuscular disease characterized by progressive muscle weakness resulting in paralysis.

8) The Flexible Brain Computer Interface (University of Rochester, USA).

Bayliss and colleagues [3.26] have performed an environmental control application in a virtual apartment that enables a subject to turn on/off a light, television set, and radio or say Hi/Bye to a virtual person. This system uses the P3 evoked potential in an immersive and dynamic Virtual Reality world. The main drawback of P3-based BCI's is their slowness. Single trial analysis may speed up recognition, but often at the cost of accuracy.

A single trial accuracy average of 85% was obtained in an environment of virtual driving. Subjects were instructed to drive in a virtual town and stop at red stop lights while ignoring both green and yellow lights. The subjects used a virtual reality helmet, and a go cart with brake, accelerator, and steering output to control the virtual car. While this choice could have caused more artifacts in the signal collection (due to turning the steering wheel and braking), most of the artifact discovered and preprocessed was due to eye movement.

4. EEG Signal Pre - Processing.

One of the main problems in the automated EEG analysis is the detection of the different kinds of interference waveforms (artifacts) added to the EEG signal during the recording sessions. These interference waveforms, the artifacts, are any recorded electrical potentials not originated in brain. There are four main sources of artifacts emission:

1. EEG equipment.
2. Electrical interference external to the subject and recording system.
3. The leads and the electrodes.
4. The subject her/himself: normal electrical activity from the heart, eye blinking, eyes movement, and muscles in general.

In case of visual inspections, the artifacts can be quite easily detected by EEG experts. However, during the automated analysis these signal patterns often cause serious misclassifications thus reducing the clinical usability of the automated analyzing systems. Recognition and elimination of the artifacts in real – time EEG recordings is a complex task, but essential to the development of practical systems.

Previous works have shown that the most severe of the artifacts are due to eyeblinks and eyeball movements. A movement of the eyeball and the eyelids causes a change in the potential field because of the existing potential difference of about 100mV between the cornea and the retina [4.1]. This change affects mainly the signals from the most frontal electrodes (Fp1 and Fp2 and also other frontal electrodes: F3, F4, F7 and F8), and induces in them many high and low frequencies, depending upon its duration and amplitude. This can be explained by the figures shown in the next page.

Fig. 4-1 shows the artifact – free bipolar EEG as recorded from standard forehead locations (Fp1 or Fp2), and its corresponding spectrum. Fig. 4-2 shows the eyeblink corrupted forehead EEG waveform and its spectrum. Fig. 4-3 shows an EEG eyeblink corrupted signal in different electrodes. It is easy to note that the eyeblinks introduce significant amount of interference in the EEG spectrum (Fig. 4-1), and also that the artifact is more visible in the two most frontal electrodes Fp1 and Fp2 (Fig. 4-3).

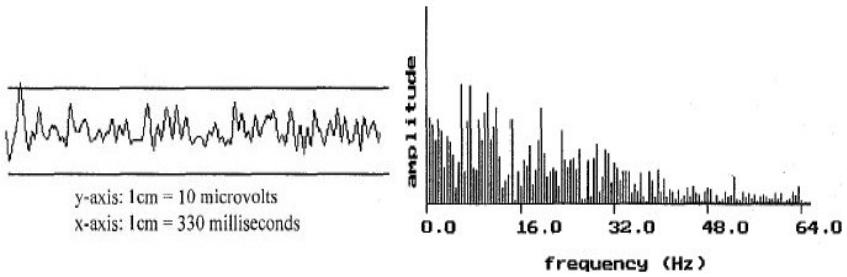

Figure 4-1. Artifact – free EEG waveform recorded by a forehead electrode, and its spectrum.

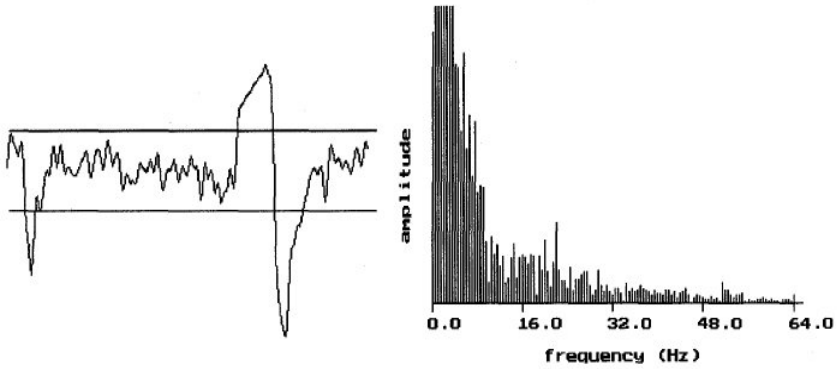

Figure 4-2. Eyeblink artifact corrupted EEG waveform recorded by a forehead electrode, and its spectrum.

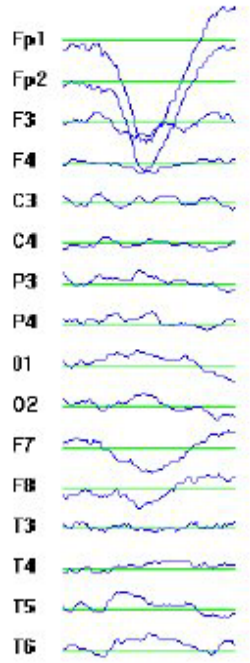

Figure 4-3. Artifact in an EEG signal.

In a clinical situation, such artifacts are rejected by visual examination of recording. There are simple criteria artifact recognition, such as those presented in [4.3], which can help in the search of an appropriate online cleaning technique. Some simple criteria, for a corrupted EEG signal, are the following:

- High amplitude of delta wave (0.5-4 Hz) in channels Fp1 and Fp2.
- Similarity of signals in channels Fp1 and Fp2.
- Rapid decline of delta wave posteriorly (the amplitude of delta wave in Fp1 and Fp2 is much higher than in other channels).

Classical methods for removing eyeblink artifacts can be classified into rejection methods and subtraction methods [4.6]:

- **Rejection methods** consist of discarding contaminated EEG, based on either automatic or visual detection. Their success crucially depends on the quality of the detection, and its use depends also on the specific application for which it is used. Thus, although for epileptic applications, it can lead to an unacceptable loss of data, for others, like a Brain Computer interface, its use can be adequate.

- **Subtraction methods** are based on the assumption that the measured EEG is a linear combination of an original EEG and a signal caused by eye movement, called EOG (*electrooculogram*). The EOG is a potential produced by movement of the eye or eyelid (Fig. 4-4). The original EEG is hence recovered by subtracting separately recorded EOG from the measured EEG, using appropriate weights (rejecting the influence of the EOG on particular EEG channels).

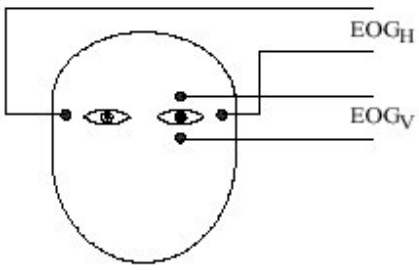

Figure 4-4. Electrooculogram electrode placement. Two EOG channels, related to vertical and horizontal eye movements (EOG_V and EOG_H), are recorded.

More recently, new methods, based on the concept of blind source separation (BSS), have been proposed in order to separate neural activity from muscle and blink artifacts in spontaneous EEG data.

In the following, four methods are presented. The first uses a BSS technique called independent component analysis (ICA). The second is a classical rejection method. The third shows an artifact recognition technique through neural networks. The last is a rejection method based on bandpass FIR filters.

4.1. Removing EEG artifacts by ICA blind source separation.

Independent component analysis (ICA) is a relatively recent method for blind source separation (BSS), which has shown to outperform the classical principal component analysis (PCA) in many applications. In particular, it has been applied for the extraction of ocular artifacts from the EEG, where principal PCA could not separate eye artifacts from brain signals, especially when they have comparable amplitudes.

ICA assumes the existence of n signals that are linear mixtures of m unknown independent source signals. At time instant i, the observed n-dimensional data vector **x**(i) = $[x_1(i)...x_n(i)]^T$ is given by the model [4.7]:

$$x_k(i) = \sum_{j=1}^{m} a_{kj} s_j(i), \qquad k = 1...n \tag{4.1}$$

$$\mathbf{x}(i) = A\mathbf{s}(i) \tag{4.2}$$

where both the independent source signals **s**(i)=$[s_1(i)...s_m(i)]$ and the mixing matrix A = $[a_{kj}]$ are unknown. Other conditions for the existence of a solution are (1) n =m (there are at least as many mixtures as the number of independent sources), and (2) up to one source may be Gaussian. Under these assumptions, the ICA seeks a solution of the form:

$$\hat{\mathbf{s}}(i) = B\mathbf{x}(i) \tag{4.3}$$

where B is called the separating matrix.

Recent experiments, as those made by Jung and colleagues [4.5], have developed new methods for removing a wide variety of artifacts based on ICA. Over EEG data collected from normal, autistic and brain lesion subjects, ICA could detect, separate, and remove contamination from a wide variety of artifactual sources in EEG records with results comparing favorably to those obtained using regression and PCA methods [4.8][4.9].

This method presents some advantages compared to other rejection methods, such as:

1. ICA separates EEG signals including artifacts into independent components based on the characteristics of the data, without relying on the availability of one or more “clean” reference channels for each type of artifact. This avoids the problem of mutual contamination between regressing and regressed channels.

2. ICA-based artifact removal can preserve all of the recorded trials, a crucial advantage over rejection-based methods when limited data are available, or when blinks and muscle movements occur too frequently, as in some subject groups.

3. Unlike regression methods, ICA-based artifact removal can preserve data at all scalp channels, including frontal and periocular sites.

Nevertheless, it is important to keep in mind that it also has some inherent limitations, such as:

1. ICA can decompose at most N sources from N scalp electrodes. Usually, the effective number of temporally-independent signals contributing to the scalp EEG is unknown, and it is likely that observed brain activity arises from more physically separable effective sources than the available number of EEG electrodes.

2. The assumption of temporal independence used by ICA cannot be satisfied when the training data set is too small, or when separate topographically distinguishable phenomena always occur concurrently in the data. In the latter case, simulations show that ICA may derive a component accounting for their joint occurrence, plus separate components accounting for their periods of solo activation. Such confounds imply that converging behavioral or other evidence must be obtained before concluding that spatio-temporally overlapping ICA components measure neuro-physiologically or functionally distinct activities.

3. ICA assumes that the physical sources of artifactual and neural activity contributing to EEG signals are spatially stationary through time. In general, there is no reason to believe that cerebral and artifactual sources in the spontaneous EEG necessarily remain stationary over time or occurrences.

4. The fact that this method needs more computations compared to a rejection approach, together with the inherently real-time nature of the EEG Brain computer Interface, makes its use a more difficult alternative.

4. 2. Artifact rejection based on peak elimination.

As previous works have shown [4.3], the presence of artifacts in EEG signals produces a rapid increase of energy in forehead locations Fp1 and Fp2. The method developed here consists of the analysis of these two channels by small overlapping windows, in order to check if the energy of the signals surpasses an established blink threshold. In case it does it, the samples coming from the corrupted signal are rejected from all the EEG signals.

Despite the simplicity of this method, the results obtained have been satisfactory enough to consider it as an initial option for a real-time Brain Computer Interface. It is easy enough to be implemented on a low complexity signal processing platform. Nevertheless, this method has the inconvenience of rejecting some non-corrupted data in other scalp channels, as well as in the frontal channels.

With the purpose of improving the data preservation, we have developed a similar system based on a quadratic Time Frequency Representation of the signal. This analysis

takes advantage of the high resolution of this technique in time and frequency, for establishing, after an appropriate training, the differences between a corrupted EEG signal and a non-corrupted EEG signal, in order to be able of distinguish and reject the eyeblink artifact. This technique, which is based on energy distributions, is an alternative to the classical artifact rejection method presented here, and it should be considered in a future work.

4. 3. Blinking artifact recognition using artificial neural network.

The method proposed by Bogacz and colleagues, used a neural based approach to find artifacts in EEG signals [4.4]. The input to the neural network was not a raw sampled signal, but different coefficients computed for a window of one second of the signal, expressing some characteristic properties of blinking artifacts. 41 coefficients were designed. Some of them were designed by the authors and were based on their knowledge about the artifact recognition, and a total of 14 were chosen by terms of sensitivity and correlation. A large training set including coefficients for over 27000 windows was used, containing different kinds of blinking artifacts, pathological and proper waves, and artifacts caused by other sources (e.g. jaw, muscle). Afterwards, three classification algorithms were tested and compared: k-neighbors, RBF networks and back propagation networks. The lowest classification error (1.40%) was obtained for the back propagation network, with a classification time of the test set (6227 windows) of 2 seconds [4.4].

This method achieves high classification accuracy thanks to two factors:

- Large training set containing different kinds of EEG waves.
- The coefficients delivered to the network's inputs, express the characteristic features of artifacts, since they encode large amount of domain expert's knowledge.

Unfortunately, the first factor can be problematic in the use of a Brain computer Interface.

4. 4. Artifact rejection based in bandpass FIR filters.

The method proposed by Gupta and colleagues used a fixed bandpass FIR filter, followed by a subject specific eyeblink threshold, in order to remove the eyeblink and eyeball movement artifacts. This technique, whose block diagram can be seen in Fig. 4-5, consist of [4.1]:

1. Pass the raw EEG samples obtained from analog-to-digital converter through a digital bandpass filter (BPF) to remove slow baseline drift.
2. Determine the blink threshold (Vt) for specific subject in brief training session.
3. Compare the absolute sample value with Vt.
4. If the value is exceeded then remove N samples from the vicinity of zero crossing (N/2 on either side of treshold crossing).
5. Shift the following N samples to fill up the gap created by blink removal. These gaps will, otherwise, grossly distort the spectrum.

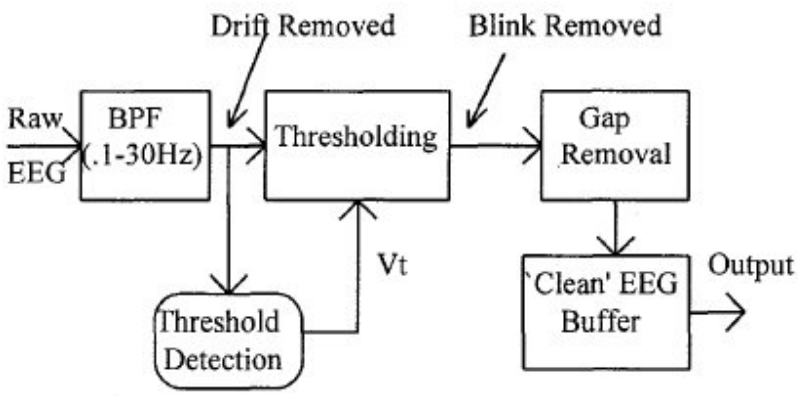

Figure 4-5. Scheme of the proposed system.

The experiments carried out through this scheme, for Fp1 and Fp2 electrodes location, provided interesting results in eyeblink artifact rejection. This method presents the advantage of working even under baseline drift artifacts conditions, and also is easy enough to be implemented on a low-cost digital signal processor, on a real – time system. Nevertheless, it fails if the blink rate is unnaturally high, and the training session for each individual is quite long: 30 sec (6 eyeblinks on a average for a normal subject).

5. EEG Signal Classification.

5.1. Introduction.

Oscillatory states are the most remarkable features of EEG activity, because they reflect not only the synchronization of massive numbers of neurons but also a temporally ordered rhythmicity of activation [5.6]. Different oscillatory patterns may be indicative of different information processing states, and it has been proposed that the oscillatory patterns play an active role in these states [5.6], [5.7]. According to this view, the rhythmic synchronization during oscillatory states can serve to enhance perception, learning, and the transmission of neuronal signals between different regions of the brain.

Traditional spectral analysis tools are not the best options to quantify the different oscillatory activities in the EEG, since the neural processes that generate the EEG are intrinsically dynamic. Indeed, there are transient changes in the power or peak frequency of EEG waves which can provide information of primary interest. The non-stationary nature of the EEG signals makes it necessary to use methods which are able to quantify their spectral content as a function of time. Time-frequency representation (TFR) methods are well suited as tools for the study of spontaneous and induced changes in oscillatory states, and we will be used here with this purpose in mind.

5.2. Feature extraction trough Time – Frequency Analysis.

In this chapter, we will explore the application of the time-frequency representation tools presented in Annex 2, to see which is more suitable for EEG signal classification. The best will be the one that maximizes the interclass variation and minimizes the intraclass variation in a time-frequency basis.

Five different tasks were presented for classification at the beginning of this project: multiplication problem solving, geometric figure rotation, mental letter composing, visual counting, and a baseline task where the subject was instructed to keep relax and think about nothing in particular. For three of these five tasks, good classification results had been obtained with AR models in previous works [5.10][5.11].

The objective of this project was centered in the search of a time-frequency method, which allows us to classify in half-second the two more problematic tasks, “rotation” and “letter”, and further study the possibility of extension to all the different tasks.

5.2.1. Short-Time Fourier Analysis: The Spectrogram.

The spectrogram is the squared magnitude of the windowed short-time Fourier transform. It considers the squared modulus of the STFT to obtain a spectral energy density of the locally windowed signal $x(u)h^*(u - t)$:

$$S_x(t, f) = \left| \int_{-\infty}^{\infty} x(u)h^*(u - t)e^{-j2\pi fu} du \right|^2$$

where h(t) is a short time analysis window located around $t = 0$ and $f = 0$.

Thus, we can interpret the spectrogram as a measure of the energy of the signal contained in the time-frequency domain centered on the point (t, f).

In the image below (Fig 5-1), the spectrograms of the five mental tasks are represented for the electrode P4, in order to see if there is an interclass variation big enough to classify them through this procedure.

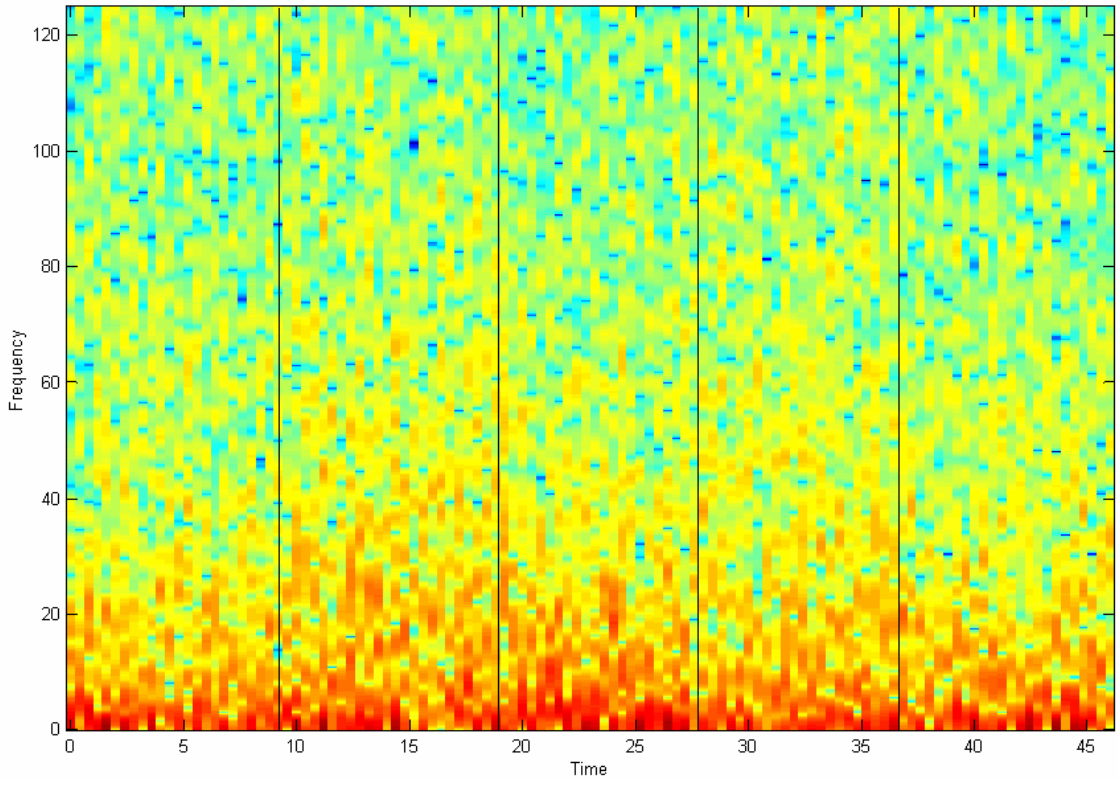

Figure 5-1. Spectrogram for the five tasks (baseline, multiplication, counting, rotation and letter). P4 electrode is considered. Five signals, one for each task, of 9-10 seconds of duration have been concatenated in a unique signal. Each signal was originally of 10 seconds, but artifacts have been rejected using the method exposed in chapter 4.2. Time runs horizontally and frequency (Hz) vertically, and colors indicate energy level.

There are no substantial differences that cleanly predict an accurate classification between the five tasks, but hopefully, we can see that the energy is distributed in different ways for each task.

Other spectrograms have been studied, using all the electrodes and a considerable amount of signals, but the same results have been obtained. It is visible that most of the EEG signals energy is concentrated in the first 30 Hz, where the most important EEG waves are supposed to be (alpha, beta, theta, delta, …), but the differences between the tasks are not very significant.

5.2.2. Quadratic Time – Frequency Representations Analysis.

The success of EEG signal analysis essentially relies on the quality and relevance of the information extracted from raw records. As can be see in Annex 2.3, the time-frequency representation of a signal is not unique. There are many different TFRs which can describe a same data, and our purpose here is find the most efficient.

Under this point of view, we will focus our attention in two energy representations: the Wigner-Ville distribution, and the Ambiguity Function.

The Wigner-Ville distribution

The Wigner-Ville distribution can be considered as the fundamental quadratic Time Frequency Representation. This fact, and its large number of desirable properties, makes its study a good starting point.

Fig. 5-2 shows the average Wigner-Ville distribution obtained for the two problematic tasks, “rotation” and “letter”, taking the channel which belongs to P4. As we can appreciate, there are some differences between the two classes. If we compare the average Wigner-Ville distributions with the WVD of a single signal in each class (Fig. 5-3), we can observe an intra class variation, but also the maintenance of the interclass differences. This behavior has been repeated in all electrodes with more or less similarity. This fact can invite us to believe in a possible classification over the time-frequency plane, since the WVD can be improved with an optimal kernel that increases these visible differences.

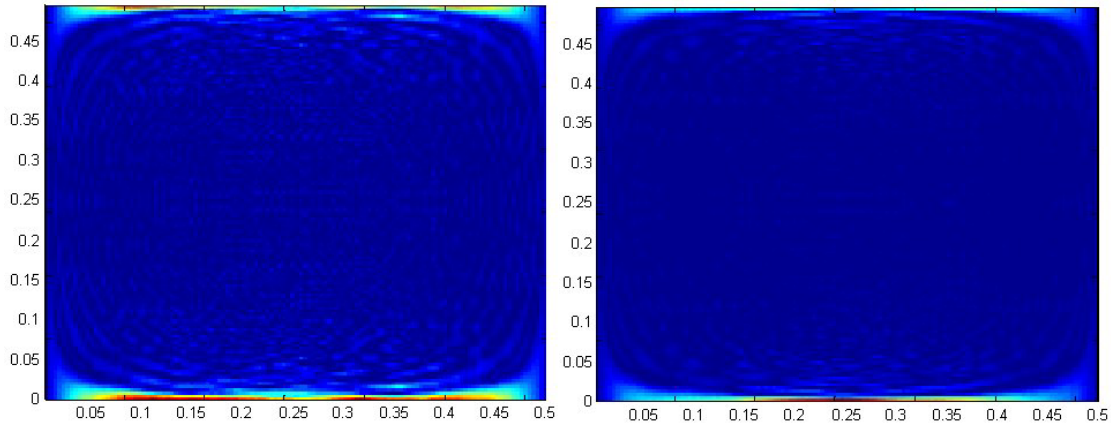

Figure 5-2. Wigner-Ville average distribution of the task "rotation" (left) and "letter" (right).
P4 electrode is considered. The average has been obtained over 110 signals of half-second for each class. Signals do not contain artifacts. Time runs horizontally and frequency (Hz) vertically, and colors indicate energy level.

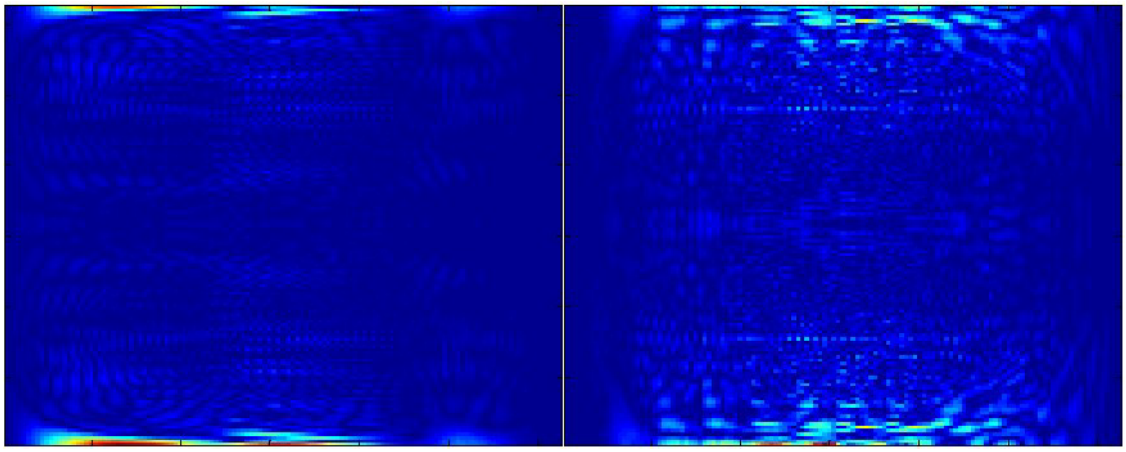

Figure 5-3. Wigner-Ville distribution for two signals of half-second from the task "rotation" (left) and "letter" (right).
P4 electrode is considered. Signals do not contain artifacts. Time runs horizontally and frequency (Hz) vertically, and colors indicate energy level.

The Ambiguity function

A function of particular interest is the inverse Fourier transform of the Wigner-Ville distribution, which is called the (symmetric) *ambiguity function* (AF) (see Annex 2.3). It presents time and frequency shift invariance in its module, which is a suitable property in the study of spontaneous EEG.

In the figure below (Fig. 5-4), the average Ambiguity Functions of the tasks “rotation” and “letter” have been depicted for the electrode P4. As we can appreciate, there are certain interclass differences that invite us to think in a possible classification over the Doppler-Delay plane.

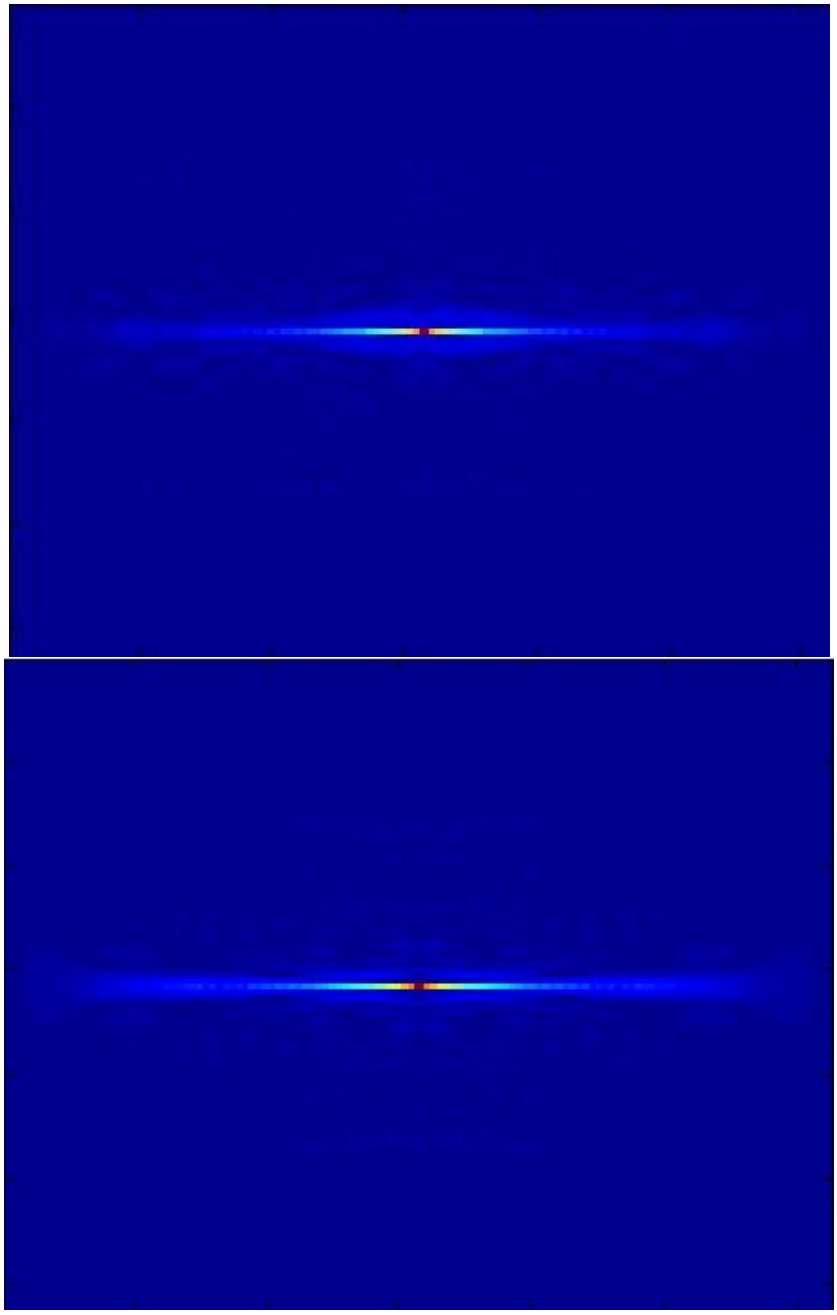

Figure 5-4. Average ambiguity function of the task “rotation” (top) and “letter” (bottom).
P4 electrode is considered. The 60 signals, through which the average has been calculated, have a duration of half-second and do not contain artifacts. Delay runs horizontally and Doppler vertically, and colors indicate energy level.

Similar results are obtained when representing the AFs of other electrodes. There is a visible difference between all the classes in the ambiguity domain (we can see the representation of four of them for the electrode O1 in Fig. 5-5).

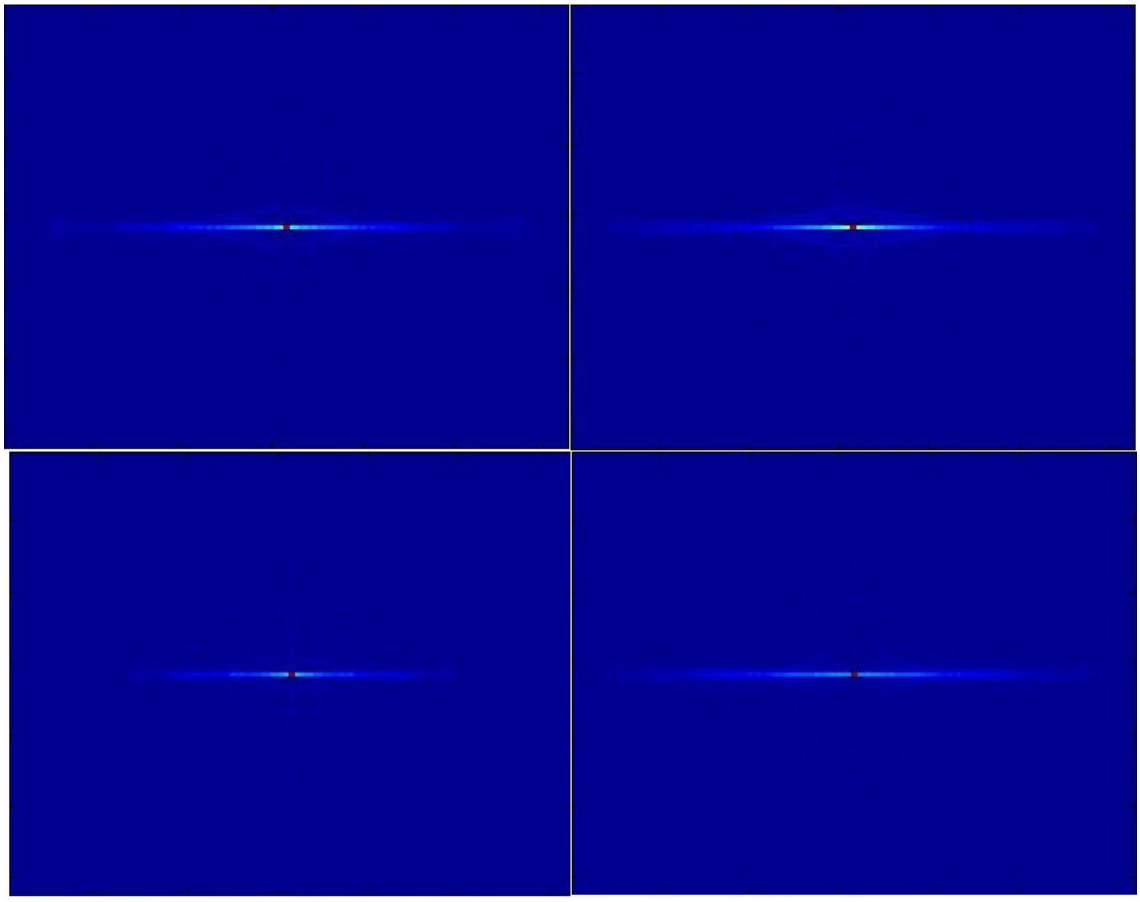

Figure 5-5. Average ambiguity function of four tasks (from left to right, and up to down: baseline, multiplication, counting and rotation).
O1 electrode is considered. The sixty signals, through which the average has been calculated, had a duration of half-second and do not contain artifacts. Delay runs horizontally and Doppler vertically, and colors indicate energy level.

As it happened with the Wigner-Ville distribution, there is an intra-class variation when comparing the AF of a single signal of half-second (see next page: Fig. 5.6). Nevertheless, a similar behavior is repeated.

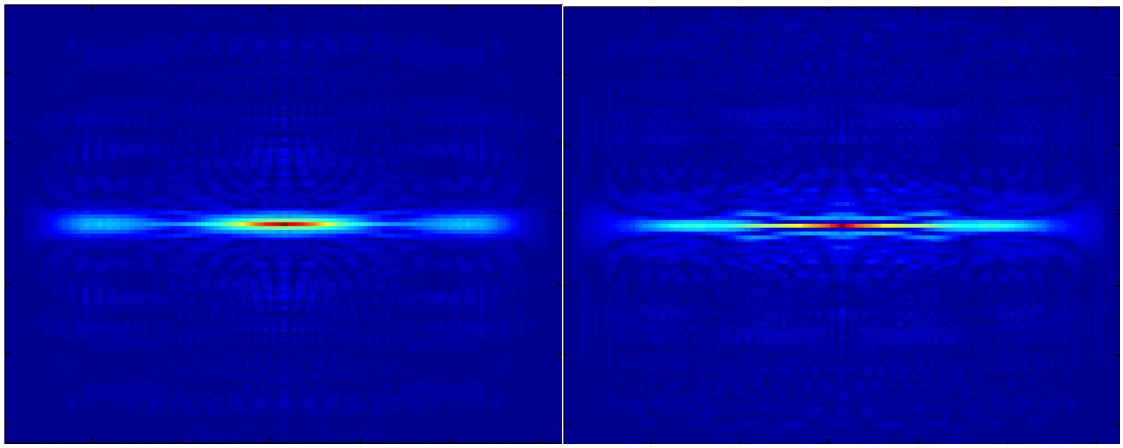

Figure 5-6. Ambiguity function for a single signal of the tasks “rotation” (left) and “letter” (right). P4 electrode is considered. The signals have a duration of half-second and do not contain artifacts. Delay runs horizontally and Doppler vertically, and colors indicate energy level.

After a preliminary qualitative observation of the EEG energy distributions, we can conclude that an acceptable classification is viable in the Time-Frequency and Doppler-Delay planes. In the next chapter, we will discuss the convenience of using them, and propose a classification method which takes advantage of these visible interclass differences.

5.3. Time – Frequency Methods for EEG signal Classification.

Time – Frequency Representations (TFRs) are powerful tools for analysis and thus widely used in signal processing. Their use for the classification of non-stationary signals has been explored in previous works [5.1][5.3][5.6], distinguishing two main families of methods: the first, known as **parametric or iterative**, requires the knowledge of the statistics of the signals to classify. The second, called "**non – iterative or empirical**", does not need this information.

The parametric or iterative methods have been firstly developed within the framework of the noisy signal detection (which is a particular case of classification). The realization of an optimal test is well known, but it needs the accurate information from the signal statistics and noise. This idea has been explored by several authors before, and it has been proven [5.2] that it can be expressed in the time-frequency plane, leading the basis of the method to an optimal expression of a kernel (core) in the Cohen's class, a distance and a rule of decision.

The non – iterative or empirical methods consist of defining the procedure of classification without using the statistical model of the signals. Approaches of this type are necessarily empirical, and that's why we have a wide variety. These methods can be interpreted also, as a search of discriminate parameters in a time-frequency plane.

Both families assume the possession of a training set for each class as the unique usable information, and try to classify the signals by a discrimination metric in the time-frequency plane.

In the development of this project, two methods based on Time – Frequency Representations, one of each family, were considered in order to classify the two given mental classes, "rotation" and "letter". After a conscientious investigation, the non – iterative method was finally selected, not only because previous studies had shown that it provided a nearly optimal solution, but also because the iterative required an initial step based on the non-iterative method.

5.3.1. Non – Iterative Method.

A classification algorithm usually is composed of a certain space of representation, and a rule of decision which assigns an individual test signal to a determined class with the aid of a discriminant function (normally a distance). The empirical nature of this method makes it necessary to search for a discriminant plane, in which we can extract specific parameters. In the present framework, there are two possible discriminant planes, the time-frequency plane and the ambiguity plane, which can be used for the development of this method.

As we have said in previous chapters, the inherent real-time characteristic of the Brain Computer Interface forces the use of an algorithm, which enables online signal processing. Although the time-frequency plane, belonging to the Cohen's class, is a discriminant plane from which we can extract useful discriminant attributes, the ambiguity plane is preferred due to its time and frequency shift invariance, which is an interesting property in the study of spontaneous EEG.

The use of the ambiguity plane for signal classification has been already studied [5.3][5.4], and is based on the utilization of the Fisher Contrast.

The algorithm: classification between two classes

The procedure of this method consist of determining the coordinates of a number of highest contrast points between two given Time Frequency Representations in the ambiguity plane, in order to compare them with the coordinates of a test AF through the measurement of a non-Euclidean distance.

1. Calculate the Fisher Contrast for the training sets of the two classes in the ambiguity plane *(Doppler (ξ), Delay (τ))*;

$$K_{Fisher}(\xi,\tau)=\frac{\left|\overline{A_1}(\xi,\tau)-\overline{A_2}(\xi,\tau)\right|^2}{\overline{\overline{A_1}}^{2}(\xi,\tau)+\overline{\overline{A_2}}^{2}(\xi,\tau)} \tag{5.1}$$

where the mean AF of each class is given by:

$$\overline{A_i}(\xi,\tau)=\frac{1}{n_{tot}}\sum_{j=1}^{n_{tot}}A_{x_i{}^j}(\xi,\tau) \tag{5.2}$$

i = number of class.
n_{tot} = total number of signals in the training set.
$A_{x_i{}^j}$ = AF of a single signal x^j_i of the training set belonging to the class i.

and the variance AF of each class is:

$$\overline{\overline{A_i}}^{2}(\xi,\tau)=\frac{1}{n_{tot}}\sum_{j=1}^{n_{tot}}(A_{x_i{}^j}(\xi,\tau)-\overline{A_i}(\xi,\tau)) \tag{5.3}$$

2. Fix a number of points: N_{point}.

3. Determine the coordinates of the N_{point} $\{(\xi, \tau)_1,\ldots, (\xi, \tau)_{Npoint}\}$ of highest contrast.

4. Classify each signal comparing its Ambiguity Function in the N_{point} $\{\{(\xi, \tau)_1,\ldots, \{(\xi, \tau)_{Npoint}\}$, with the mean AF of the training set of each class in the same points, making use of the Mahalanobis distance.

As we increment the number of points considered, N_{point}, the number of highest contrast coordinates will be also increased. Consequently, there exists an optimal N_{point}, from which the classification rate begins to get worse. As the number of points N_{point} become larger, the following selected coordinates do not represent any contrast between the classes.

We can interpret the N_{point} selected in the Doppler-Delay plane, as an adaptable binary function, which can be also seen as an optimal binary kernel, that masks the ambiguity function of a training set of signals. Fig. 5-4 represents the average AF, through which the Fisher Contrast must be computed, for the tasks rotation and letter, considering the channel P4. Fig. 5-7 shows the binary core that results from the Fisher Contrast for $N_{point} = 100$.

This method has the added advantage of reducing the computational cost by four ($N_{point}/4$), because the ambiguity function presents symmetry with respect to the origin ($\xi = 0$, $\tau = 0$), and its module presents also symmetry with respect to the Doppler and Delay axes. Therefore, it is enough to consider one quadrant of the ambiguity plane.

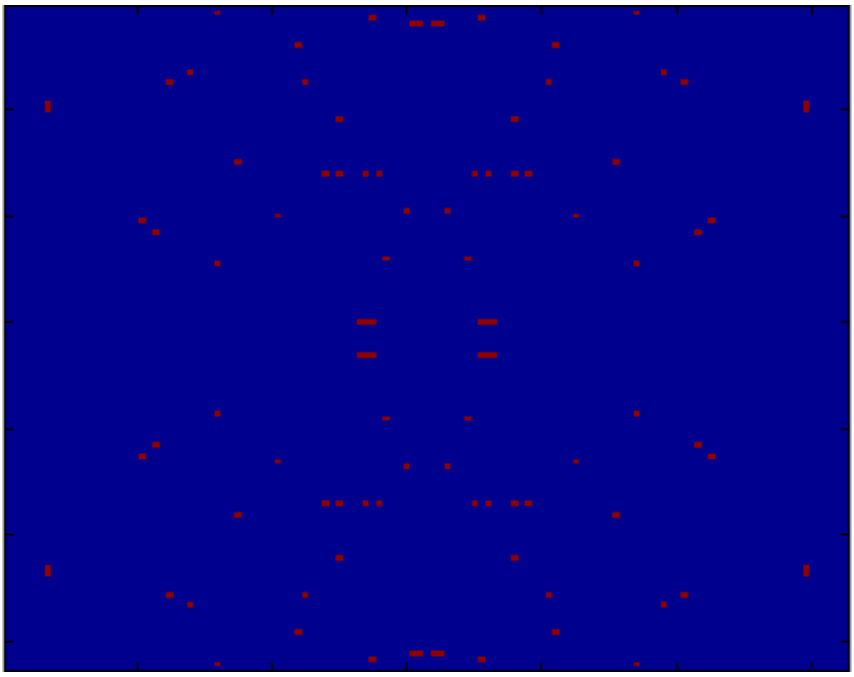

Figure 5-7. Fisher Contrast of the training set of the tasks rotation and letter.
P4 electrode is considered. The training set comprehends an amount of 30 non-corrupted half-second signals for each class. Delay runs horizontally and Doppler (Hz) vertically. The colored points indicate the coordinates of the most contrast points.

The Mahalanobis distance.

The squared Mahalanobis distance, is a distance measurement in cluster analysis where a scale independence is needed. It associates the correlation between parameters and normalizes each parameter to zero mean and unit variance by using the covariance matrix in the distance calculation. Its expression given by:

$$d_{Mahalanobis}(z_i, z_j) = \sqrt{(z_i - z_j)^T \sum^{-1} (z_i - z_j)} \qquad (5.4)$$

where Σ^{-1} is the inverted covariance matrix, and z_i, z_j are the data points for which the distance is calculated.

Figure 5-8. Visualization of a data set to demonstrate the usage of the Mahalanobis Distance.

We use this distance measurement mostly to calculate the distance between the mean of a cluster *i* and a single data point z_j. The expression for the distance is then given by:

$$d_{\sum_i}(z_j, \bar{z}_i) \tag{5.5}$$

where $\bar{z}_i$ is the mean of cluster *i*, $\sum_i$ the covariance matrix of cluster *i*, and z_j is the data point the distance is calculated for. The Mahalanobis distance is then used to identify the closest point to a cluster or group of points (Fig. 5-8), or to calculate the distance and separation of two clusters.

The relevance of the Mahalanobis distance is shown in Fig. 5.8. The data set is shaped as a rectangle with the main axis parallel to the abscissa. The rectangle is compressed on its minor axis. The center of the data set is marked as $\overline{Z}$. The data points z_1 and z_2 are emphasized. Obviously, the data point z_2 would be closer to $\overline{Z}$ if the Euclidean distance d_I is used, but it does not belong to the cluster. On the other side, the further distanced data point z_1 is within the cluster. The importance to use a distance measurement which is taking the shape of the cluster into consideration, is shown in this example, as well as the disadvantage of the Euclidean distance. This is the reason for the use of the Mahalanobis distance, by considering the standard deviations of the AF means of the training samples

The Generalized Fisher Contrast: N-class classification

We can extend the idea of the Fisher Contrast for its use in an N-class classification problem, trying to generalize the equation 5.1. The point of view of the Fisher contrast is to optimize the representation space in order to maximize the value of $K_{Fisher}(\xi,\tau)$, by increasing the distance between the mean of the N classes, while reducing the intra-class dispersion.

Thus, if we consider in the numerator all the possible combinations among the N classes, and we divide them by the sum of the N means, we obtain a contrast which emphasizes the differences among the N classes. The generalized Fisher Contrast is:

$$K_{Fisher}(\xi,\tau) = \frac{\sum_{\substack{i=1 \\ i<j}}^{N} \left| \overline{A_i}(\xi,\tau) - \overline{A_j}(\xi,\tau) \right|^2}{\sum_{i=1}^{N} \overline{\overline{A_i}}^2(\xi,\tau)} \tag{5.6}$$

where the mean AF of each class is given by:

$$\overline{A_i}(\xi,\tau) = \frac{1}{n_{tot}} \sum_{j=1}^{n_{tot}} A_{x_i^j}(\xi,\tau) \tag{5.7}$$

i = number of class.
n_{tot} = total number of signals in the training set.
$A_{x_i^j}$ = AF of a single signal x^j_i of the training set belonging to the class i.

and the variance AF of each class is:

$$\overline{\overline{A_i}}^2(\xi,\tau) = \frac{1}{n_{tot}} \sum_{j=1}^{n_{tot}} (A_{x_i^j}(\xi,\tau) - \overline{A_i}(\xi,\tau)) \tag{5.8}$$

The generalized algorithm of classification is similar to the two-class classification algorithm. Once we have the coordinates of the N_{point} $\{(\xi, \tau)_1,\ldots, (\xi, \tau)_{Npoint}\}$ of highest contrast, we just have to compare in those N_{point} the AF of a signal to be classified with the mean AF of the training set of each class, making use of the Mahalanobis distance, and to assign the signal to the class with the smallest distance.

6. Results.

In this section, we will present the results obtained using the non-iterative time-frequency classification method based on the application of Fisher Contrast over the ambiguity domain.

All the data used in this project was obtained previously by Zak Keirn at Purdue University for his work on his Masters of Science thesis in the Electrical Engineering Department at Purdue [6.1]. The recording procedure was the following. The subject was seated in an Industrial Acoustics Company sound controlled booth with dim lighting and noiseless fans for ventilation. An Electro-Cap was used to record from positions C3, C4, P3, P4, O1 and O2, defined by the 10-20 system of electrode placement (chapter 2.1-Fig. 2.2). The electrodes were connected through a bank of Grass 7P511 amplifiers and bandpass filtered from 0.1-100 Hz. Data was recorded at a sampling rate of 250 Hz with a Lab Master 12 bit A/D converter mounted on a PC. Recordings were made with reference to electrically linked mastoids A1 and A2 (see Fig 2.2).

For this project, the data from seven subjects performing five mental tasks were analyzed. These tasks were chosen by Keirn to invoke hemispheric brainwave asymmetry [6.2]. The five tasks are:

1. *The baseline mental task*, for which the subjects were asked to relax as much as possible and think of nothing in particular.
2. *The math task*, for which the subjects were given nontrivial *multiplication problems*, such as 49 times 78, and were asked to solve them without vocalizing or making any other physical movements.
3. *The visual counting task*, for which the subjects were asked to imagine a blackboard and to visualize numbers being written on the board sequentially.
4. *The geometric figure rotation*, for which the subjects were asked to visualize a particular three-dimensional block figure being rotated around an axis.
5. *The letter task*, for which the subjects were instructed to mentally compose a letter to a friend or relative without vocalizing.

Subjects 1 and 2 were employees of a university and were left-handed age 48 and right-handed age 39, respectively. Subjects 3 through 7 were right-handed college students between the age of 20 and 30 years old. All were male subjects with the exception of Subject 5. Subjects performed five trials of each task in one day. They returned to do a second five trial another day. Subjects 2 and 7 completed only one 5-trial session. Subject 5 completed three sessions.

Data was recorded for 10 seconds during each task and each task was repeated ten times per session. With a 250 Hz sampling rate, each 10 seconds trial produces 2500 samples per channel. After preprocessing for artifact rejection (chapter 4.2), the resulting signals, whose duration is logically reduced, were divided into half-second segments, producing a final set for each subject and each mental task of 110 signals of 6 channels with 125 samples per channel.

A collection of 30 signals was selected for each subject and each mental task as the training set. The rest of the signals, 80 for each subject and mental task, were used for testing.

6.1. Classification between two classes: “rotation” and “letter”.

For the two-class classification problem, the data of the mental tasks “rotation” and “letter” (four and five) have been considered. Experiments based on the Fisher Contrast method were performed over the six electrodes, using a training set of 30 signals for each subject and each mental task, 60 in total, and a testing set of 80 signals for each subject and each mental task, 160 in total. Electrodes O1 and P4 have shown a better behavior, and their results are presented in Fig. 6-1 and 6-2. As we can see, the error rate obtained for the two-class classification problem approaches zero as we increase the number of points chosen in the Fisher Contrast. Logically, this tendency should reverse when the number of points chosen is too large.

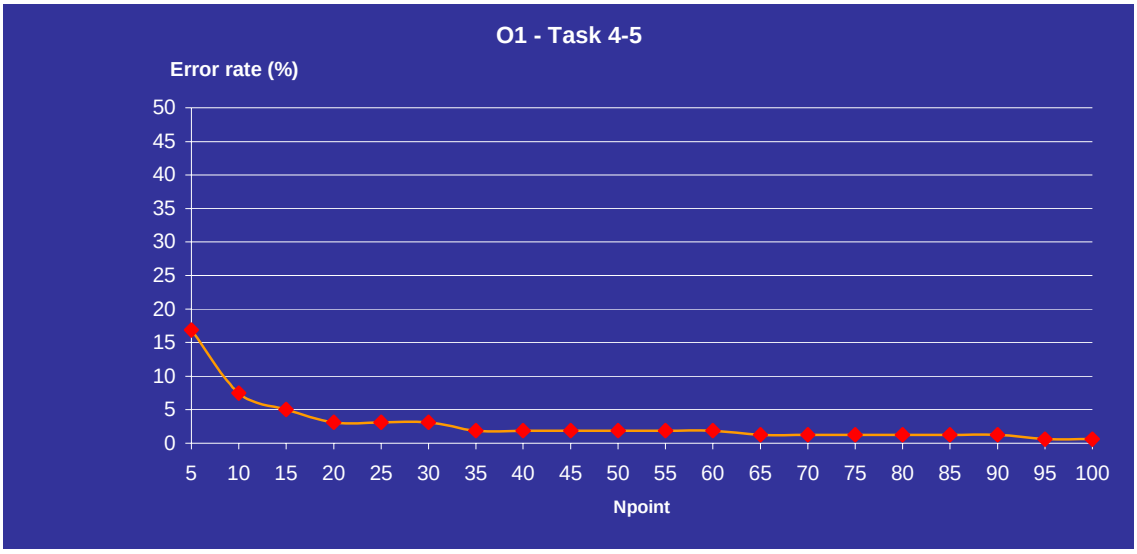

Figure 6-1. Experimental results for tasks four and five (“rotation” and “letter”) considering the channel Occipital 1.
60 signals were use for training, and 160 for test.

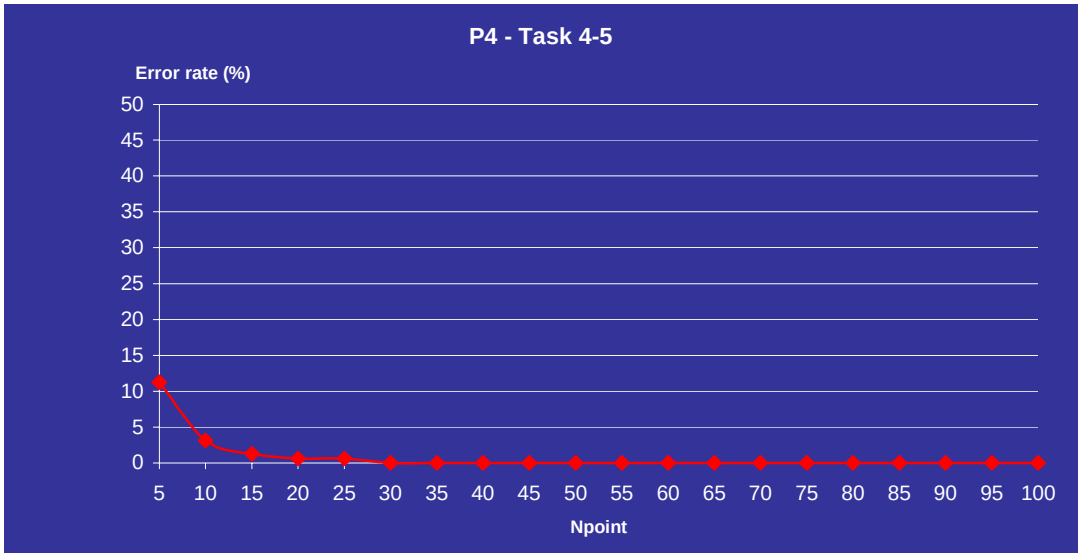

Figure 6-2. Experimental results for classification between tasks four and five ("rotation" and "letter") considering the channel Parietal 4.
60 signals were use for training, and 160 for test.

Similar results have been obtained in the two-class classification problem, when different mental tasks have been considered, as we can see for example in Fig. 6-3 for the mental tasks "multiplication" and "counting" (two and three). Electrodes P4 and O1 have shown a better behavior.

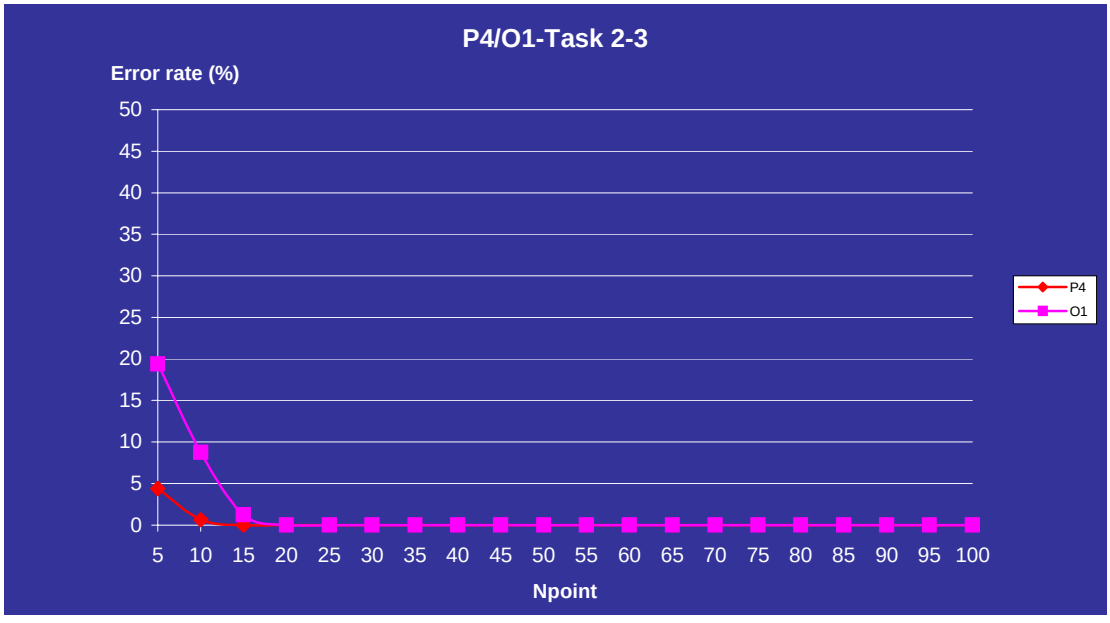

Figure 6-3. Experimental results for classification between tasks two and three ("multiplication" and "counting"), considering the channels Parietal 4 (red line) and Occipital 1 (pink line).
60 signals were use for training, and 160 for test.

6.1. Classification between five classes.

For the five-class classification problem, the data of the mental tasks “baseline”, “multiplication”, “counting”, “rotation” and “letter” have been considered. Experiments based on the generalized Fisher Contrast method have been performed over six electrodes, using a training set of 30 signals for each subject and each mental task, 150 in total, and a testing set of 80 signals for each subject and each mental task, 400 in total. Electrodes O1 and P4 have shown a better behavior, and their results are presented in Fig. 6-4 and 6-5. As we can see, the error rate obtained for the five-class classification problem approaches zero as we increase the number of points chosen in the Fisher Contrast. Logically, this tendency should reverse when the number of points chosen is too large.

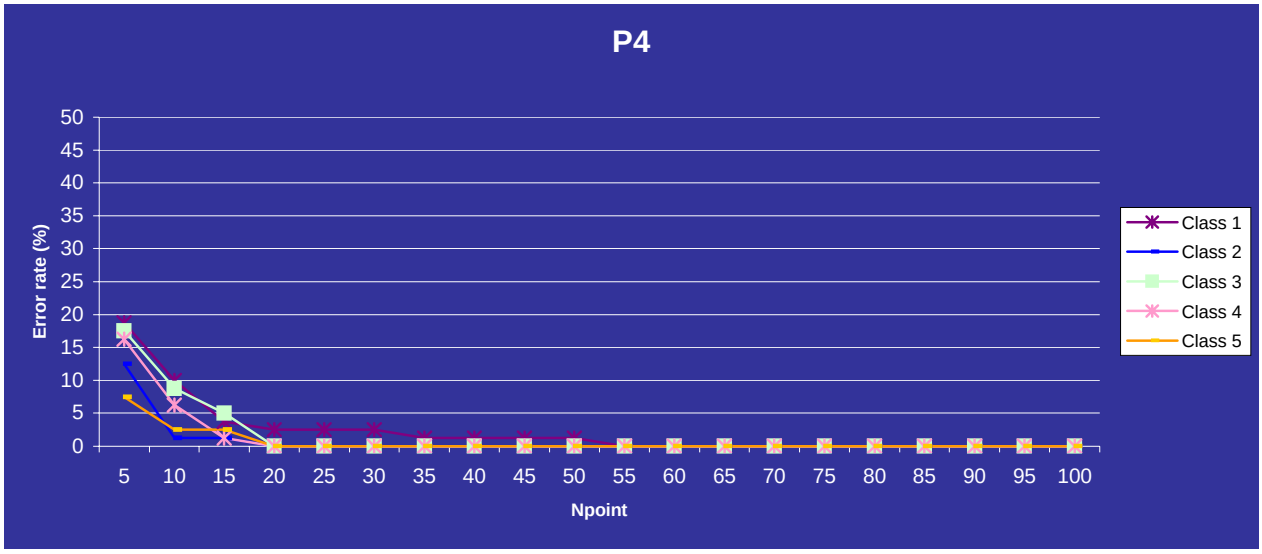

Figure 6-4. Evolution of the classification error rate with the number of points selected from the Fisher Contrast.
Experimental results are presented for the five tasks considering the channel Parietal 4.
The five tasks are “baseline” (1), “multiplication” (2), “counting” (3), “rotation” (4) and “letter” (5).
150 signals, 30 of each class, were use for training, and 400, 80 of each class, for test.

Based on these experiments we can conclude that electrode P4 provides the best results for the classification of a signal, which belongs to tasks 2, 3, 4 and 5, between all the five tasks. The electrode O1 provides the best result for task 1 classification.

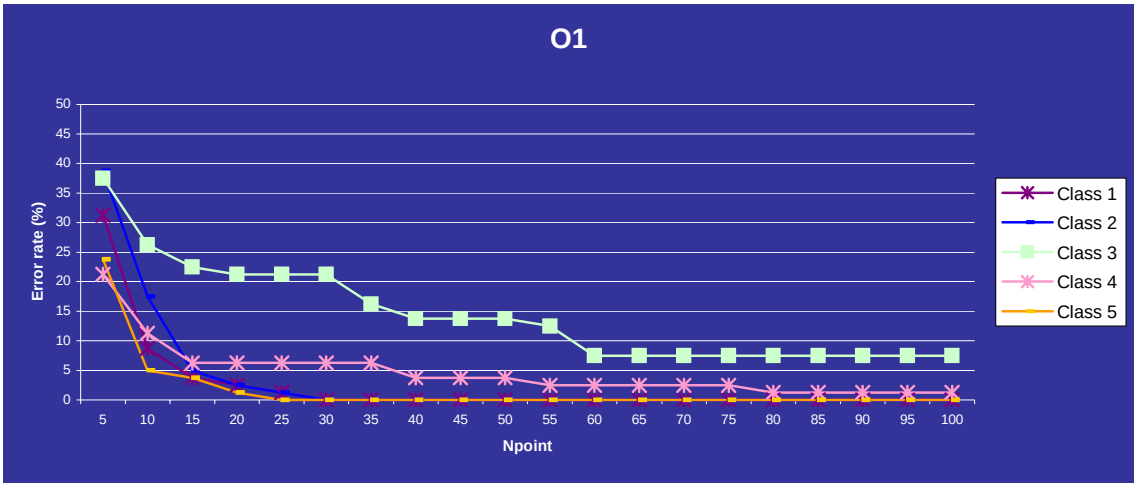

Figure 6-5. Evolution of the classification error rate with the number of points selected from the Fisher Contrast.
Experimental results are presented for five mental tasks considering the channel Occipital 1.
The five tasks are “baseline” (1), “multiplication” (2), “counting” (3), “rotation” (4) and “letter” (5).
150 signals, 30 of each class, were use for training, and 400, 80 of each class, for test.

8. Conclusions.

The role of signal processing is crucial in the development of a real-time Brain Computer Interface. Until recently, several improvements have been made in this area, but none of them has been entirely successful. The goal of creating more effective classification algorithms, have focused numerous investigations in the search of new techniques of feature extraction.

A BCI has to be useful for a wide variety of tasks, for instance, when a BCI is used as the main control device for a handicapped individual. In this study, signals from five different tasks were used as the basis for tests. Among the five tasks, multiplication problem solving, geometric figure rotation, mental letter composing, visual counting, and a baseline task where the subject was instructed to think about nothing in particular, two ("rotation" and "letter") had been problematic in a previous classification method based on autoregressive models. The discovery of a new method founded on Time Frequency Representations was of vital importance not only for these two tasks, but also for future research.

In this diploma project, we have presented a generic model of feature extraction based on time-frequency analysis, which can be effectively used, not only for classifying complex EEG signals such as those belonging to "rotation" and "letter" mental tasks, but also for a wide class of EEG signals. A new path has been opened, and only future will be able to judge if this method can be successfully applied to real-time BCI systems.

9. Present and Future.

The practical use of BCI technology depends on an interdisciplinary cooperation between neuroscientists, engineers, computer programmers, psychologists, and rehabilitation specialists, in order to develop appropriate applications, to identify appropriate users groups, and to pay careful attention to the needs and desires of individual users.

The prospects for controlling computers through neural signals are indeed difficult to judge because the field of research is still in its infancy. Much progress has been made in taking advantage of the power of personal computers to perform the operations needed to recognize patterns in biological impulses, but the search for new and more useful signals still continues.

If the advances of the 21st century match the strides of the past few decades, direct neural communication between humans and computers may ultimately mature and find widespread use. Perhaps newly purchased computers will one day arrive with biological signal sensors and thought-recognition software built in, just as keyboard and mouse are commonly found on today's units.

Annex1: Biomedical considerations.

The brain contains approximately 100 billion *neurons* [A1-1]. Each neuron may have as many as 2000 or more connections with other neurons and may receive as many as 20,000 inputs. Abstractly, a neuron is probably the most diverse, in terms of form and size, of all cells in the body; however, all neurons have in common the functional properties of integration, conduction and transmission of nerve impulses. A neuron consists of three basic parts (Fig. A1-1):

- **Cell body** (or *soma*). This main part has all of the necessary components of the cell, such as the nucleus (contains DNA), *endoplasmic reticulum* and *ribosomes* (for building proteins) and *mitochondria* (for making energy). If the cell body dies, the neuron dies.
- **Axon** - This long, cable-like projection of the cell carries the electrochemical message (nerve impulse or action potential) along the length of the cell. Depending upon the type of neuron, axons can be covered with a thin layer of *myelin*, like an insulated electrical wire. *Myelin* is made of fat, and it helps to speed transmission of a nerve impulse down a long axon. Myelinated neurons are typically found in the peripheral nerves (sensory and motor neurons), while non-myelinated neurons are found in the brain and spinal cord.
- **Dendrites** or **nerve endings** - These small, branch-like projections of the cell make connections to other cells and allow the neuron to talk with other cells or perceive the environment. Dendrites can be located on one or both ends of the cell. There are two types of dendrites, apical and basal dendrites.

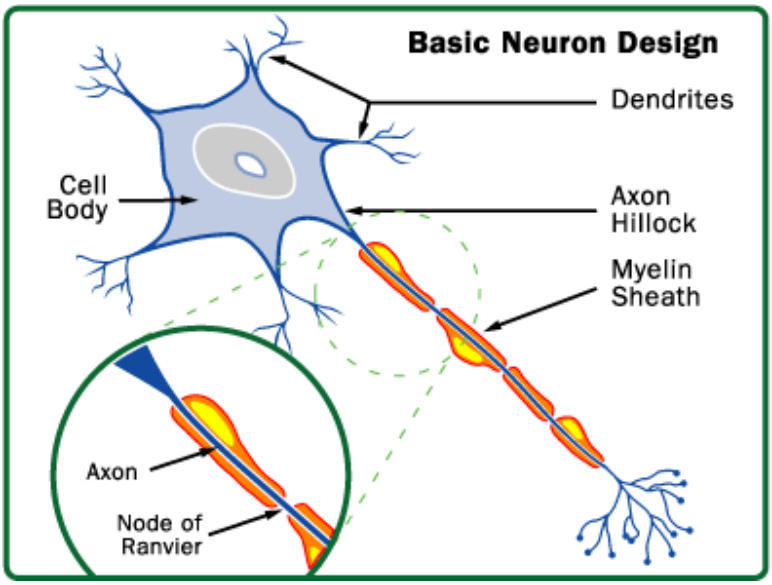

Figure A1-1. Neuron topology.
Each neuron is in contact through its axon and dentrites with other neurons, so that each neuron is an interconnecting segment in the network of the nervous system.

Neurons come in many sizes. For example, a single sensory neuron from the fingertip has an axon that extends the length of the arm, while neurons within the brain may extend only a few millimeters. Neurons have different shapes depending on what they do. Motor neurons that control muscle contractions have a cell body on one end, a long axon in the middle and dendrites on the other end; sensory neurons have dendrites on both ends, connected by a long axon with a cell body in the middle. Neurons also vary with respect to their functions:

- **Sensory neurons** carry signals from the outer parts of the body (periphery) into the central nervous system.
- **Motor neurons** (motoneurons) carry signals from the central nervous system to the outer parts (muscles, skin, glands) of the body.
- **Receptors** sense the environment (chemicals, light, sound, touch) and encode this information into electrochemical messages that are transmitted by sensory neurons.
- **Interneurons** connect various neurons within the brain and spinal cord.

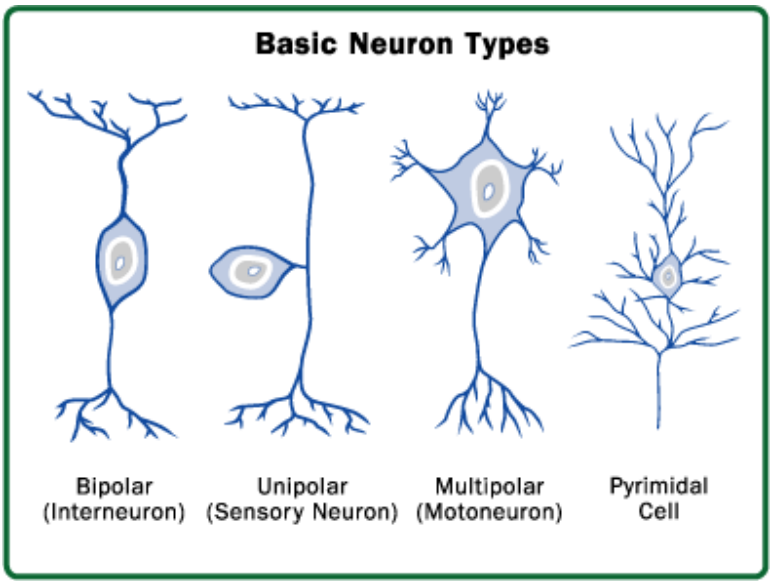

Figure A1-2. Some types of neurons: interneuron, sensory neuron, motoneuron and cortical pyramidal cell.

The *synapse*, a specialized site of contact between neurons, is of prime significance in the integrative activities of the nervous system, as the information from one neuron flows to another neuron across of it. The synapse is a small gap separating 2 neurons, and consists of:

1. A presynaptic ending that contains neurotransmitters, mitochondria and other cell organelles.
2. A postsynaptic ending that contains receptor sites for neurotransmitters.
3. The synaptic cleft: a space between the presynaptic and postsynaptic endings.

For communication between neurons, an electrical impulse must travel down an axon to the synaptic terminal.

Electric potentials are produced at the synaptic junctions, which can be localized over the axon (axoaxonic synapse), the soma (axosomatic synapse) or the dentrites (axodendritic synapse) (Fig A1.3), and reflect the communication between neurons. When a neurotransmitter binds to a receptor on the postsynaptic side of the synapse, it changes the postsynaptic cell's excitability: it makes the postsynaptic cell either more or less likely to fire an action potential. If the number of excitatory postsynaptic events are large enough, they will cause an action potential in the postsynaptic cell and the continuation of the "message." In addition to The EEG pick up this synchronized subthreshold dentritic potentials produced by the postsynaptic activity of many neurons summed [A1-2].

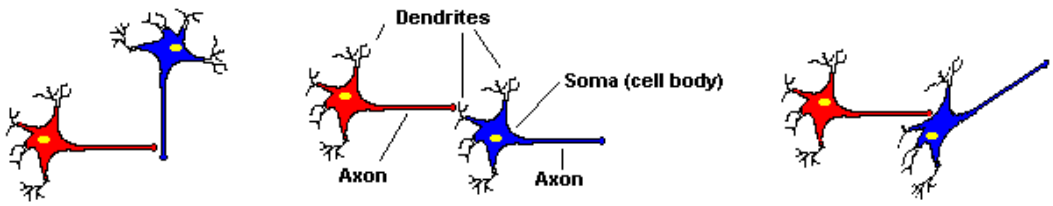

Figure A1-3. Types of synapses. From left two right: axoaxonic synapse, axodendritic synapse, and axosomatic synapse.

Not all types of brain activity have identical impact on the EEG. The depth, orientation and intrinsic symmetry of connections in the cortex are significant in it. The primary cell of importance in the neocortex is the pyramidal cell. It's known that its neurotransmitter is a potent excitatory transmitter. The pyramidal cell receives many inputs from stellate cells that are also excitatory. The pyramidal cell is different from other neurons in that it violates one of the fundamental rules of standard neurophysiology, that only axons produce action potentials which transmit information from one cell to another, and dendrites produce excitatory and inhibitory slow potentials that summate at the axon hillock where they establish the action potentials. In the case of the pyramidal cell, the apical dendrite, which is a long shaft between the basal and apical region, can actually produce action potentials, and these in turn act to amplify the powerful action potentials that now project to output systems--sensory, motor, autonomic, or integrative [A1.3]. For this reason, pyramidal cells are thought to cause the strongest part of the EEG signal.

Annex 2: Time – Frequency Analysis.

The success of EEG signal analysis essentially relies on the quality and the relevance of the information extracted from raw records. This section presents the signal processing methods related with the aim of the project, the time – frequency methods of signal analysis, used for feature extraction.

A2.1. Introduction.

The traditional analysis tools we use for the analysis of stationary signals, such as the Fourier transform, are no longer adequate for the analysis of most non –stationary signals. Instead, Time – Frequency Representations (TFRs) are more suitable. They combine time and frequency domain to yield a revealing picture of how a signal's frequency content changes with time. As different signals have diverse desirable properties that are needed in various applications, different Time – Frequency Representations are necessary for the analysis of different types of signals.

TFRs may be divided into two groups by the nature of their transforms [A2.1] [A2.2]: *linear methods* (including the Short – Time Fourier Transform) and *quadratic methods* (based on the Wigner – Ville distribution).

A2.2. Short-Time Fourier Analysis.

One of the mathematical methods with greater application in signal processing is the Fourier Transform (FT), which breaks down a signal into constituent sinusoids of different frequencies:

$$X(f) = \int x(t) e^{-2j\pi ft} dt \qquad \text{(A2.1)}$$

Another way to think of Fourier analysis is as a mathematical technique for transforming our view of the signal from time-based to frequency-based (Fig. A2-1).

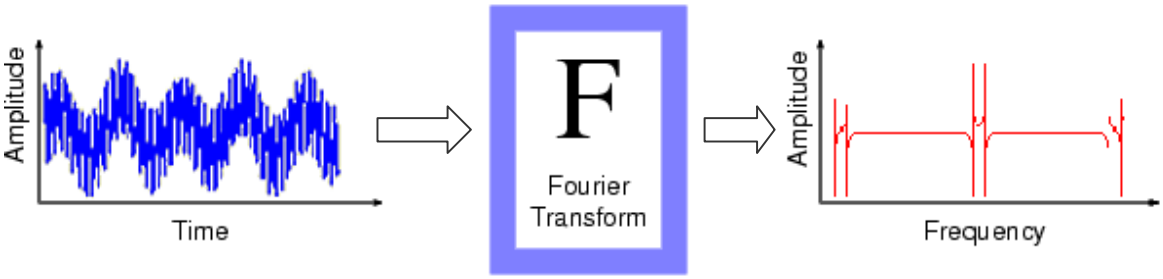

Figure A2-1. The Fourier Transform.

For many signals, Fourier analysis is extremely useful because the signal's frequency content is of great importance, but it has a serious drawback. In transforming to the frequency domain, time information is lost. When looking at a Fourier transform of a signal, it is impossible to tell when a particular event took place, because the analysis coefficients X(f) denote the distribution of the signal in the frequency domain for the entire record, that is, with no time resolution.

If the signal properties do not change much over time –that is, if it is what is called a *stationary* signal– this drawback isn't very important. However, most interesting signals, like the EEG signals, contain numerous non-stationary or transitory characteristics: drift, trends, abrupt changes, and beginnings and ends of events. These characteristics are often the most important part of the signal, and Fourier analysis is not suited to detect them.

In an effort to correct this deficiency, Dennis Gabor (1946) adapted the Fourier transform to analyze only a small section of the signal at a time. This intuitive solution consists of multiplying the signal x(τ) with a temporal window function h. The resulting transform, called the *Short-Time Fourier Transform* (STFT), is:

$$STFT(t, f) = \int x(\tau) h^*(\tau - t) e^{-2j\pi ft} d\tau \qquad \text{(A2.2)}$$

which maps the signal into a two dimensional time – frequency domain (Fig. A2-2).

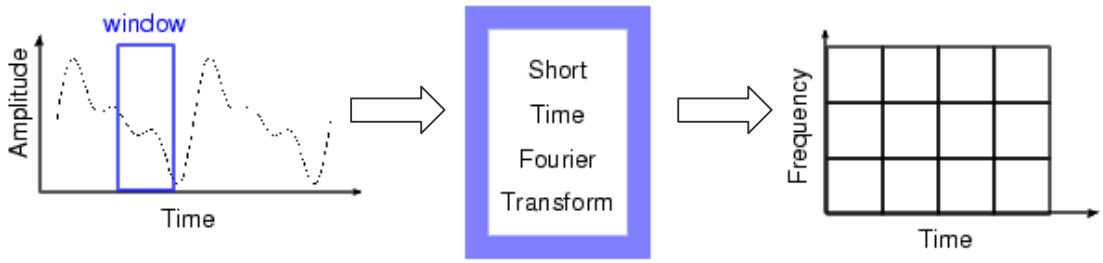

Figure A2-2. The Short Time Fourier Transform.

It is important to consider the bounds on temporal resolution Δt and frequency resolution Δf of the STFT. The time resolution of the STFT is proportional to the effective duration of the window h, as we can see considering for x a Dirac impulse. Similarly, the frequency resolution of the STFT is proportional to the effective bandwidth of the window h. Consequently, for the STFT we have a trade – off between time and frequency resolution: a good time resolution requires a short window, and a good frequency resolution requires a long window. This limitation is a consequence of the *"time – bandwidth uncertainty principle"* or the *"Heisenberg inequality"*:

$$\Delta t \cdot \Delta f \geq \frac{1}{4\pi} \tag{A2.3}$$

Therefore, the problem consists of the selection of an optimal analysis window for each application.

A2. 3. Quadratic Time – Frequency Representations.

The main disadvantage of linear time – frequency transforms is that the time – frequency resolution is limited by the Heisenberg bound, which is due to the imposition of a local time window.

In contrast with the linear TFRs, the quadratic TFRs distribute the energy of the signal over the time – frequency domain. As there are many time-frequency energy distributions, there are also many TFRs for the same signal. In other words, many different TFRs can explain the same data. One of the characteristics of the quadratic TFRs is the absence of a windowing function, which yields a very high – dimensional TFR that offers superior resolution when compared to any linear method.

The Wigner-Ville Distribution

A time-frequency energy distribution which is particularly interesting is the Wigner-Ville distribution (WVD), which is defined as:

$$WVD_x(t, f) = \int x(t + \tau/2)x^*(t - \tau/2)e^{-2\pi ft}\, d\tau \tag{A2.4}$$

In some sense, we can say that the WVD is the fundamental quadratic Time Frequency Representation [A2.1], because it is possible to build all the shift covariance TFRs from it. Unfortunately, this distribution is negatively affected by nonlinear artifacts called *cross-components*, which can obscure the true signal *auto-components* with irrelevant information. To illustrate these features, we present below (Fig. A2-3) a bat chirp signal, which is the digitized 2.5 microsecond echolocation pulse emitted by the Large Brown Bat, and its Wigner-Ville distribution. As we can see, the time-frequency image of the signal clearly exposes the frequency variation over time.

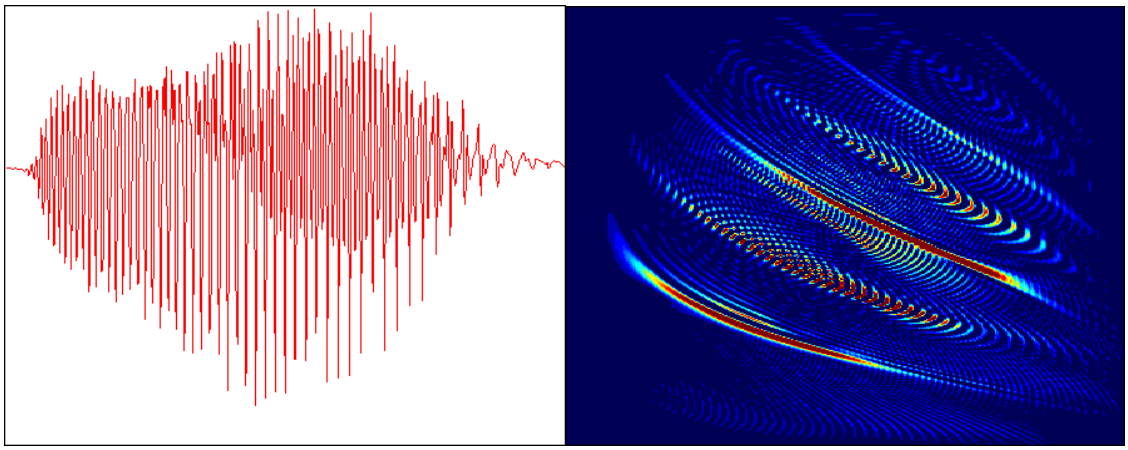

Figure A2-3. Bat chirp signal and its Wigner- Ville distribution.
In the left image, time runs horizontally and amplitude vertically. In the right image, time runs horizontally and frequency vertically, and the colors indicate energy level.

While the hyperbolic nature of the chirp is evident in the WVD image, the copious cross-components would complicate a more detailed analysis. In general, WVD cross-components have the following properties:

- A WVD cross-component appears between each pair of WVD auto-components.
- Each WVD cross-component oscillates in time-frequency with a spatial frequency inversely proportional to the auto-component separation distance.

The Ambiguity Function

A function of particular interest, is the inverse Fourier transform of the Wigner-Ville distribution, which is called the (symmetric) *ambiguity function* (AF):

$$A_x(\xi,\tau) = \int x(u+\tau/2)x^*(u-\tau/2)e^{-2\pi\xi u}\ du \qquad \text{(A2.5)}$$

This function is a measure of the time-frequency correlation of a signal, that is, the degree of similarity between x and its translated versions in the time-frequency planee. Unlike the variables t and f, which are "absolute" time and frequency coordinates, the variables τ and ξ, which are respectively called *Delay* and *Doppler*, are "relative" coordinates.

This interpretation of the Ambiguity Function as a TF Correlation [A2.4] can be seen in Fig. A2-4. The Expected Ambiguity Function (EAF) is an intuitively reasonable measure for the statistical correlation between two TF points (t_1, f_1) and (t_2, f_2)

$$C_x(t_1, f_1; t_2, f_2) = E\left\{\langle x, g_1\rangle\langle x, g_2\rangle^*\right\} \qquad \text{(A2.6)}$$

where $g_1(t)$ and $g_2(t)$ are two normalized test signals TF-located about (t_1, f_1) and (t_2, f_2), respectively (see Fig. A2-4(a)). The inner product $\langle x, g_1 \rangle = \int x(t) g_i^*(t) dt$ measures the content of $x(t)$ about the TF point (t_i, f_i). It is shown that the TF correlation $C_x(t_1, f_1; t_2, f_2)$ can be derived from the EAF $EA_x(\tau, \nu)$ as

$$C_x(t_1, f_1; t_2, f_2) = \langle EA_x, A_{g1g2} \rangle = \int_\tau \int_\nu EA_x(\tau, \nu) A_{g1g2}(\tau, \nu) d\tau d\nu \quad \text{(A2.7)}$$

where $A_{g1g2}(\tau, \nu)$ is the cross-AF of the test signals $g_1(t)$ and $g_2(t)$.

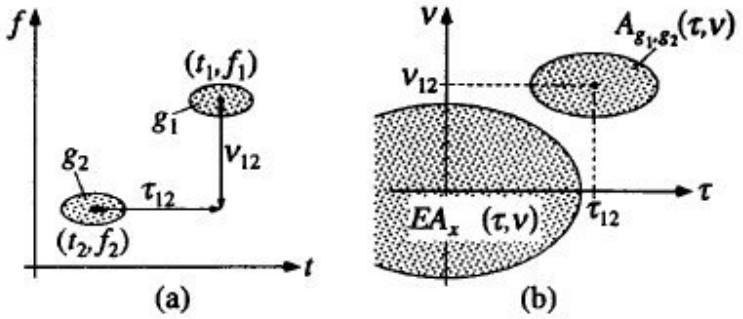

Figure A2-4. TF correlation interpretation of the Expected Ambiguity Function (EAF): (a) TF plane, (b) TF lag plane.

As the AF is the dual of the WVD in the sense of the Fourier transform, for the AF, a dual property corresponds to nearly all the properties of the WVD. Among these properties, the most important are [A2.2]

- Marginal properties:
  The temporal and spectral auto-correlations are the cuts of the AF along the τ-axis and ξ-axis respectively:

  $$r_x(\tau) = A_x(0, \tau) \text{ and } R_x(\xi) = A_x(\xi, 0) \quad \text{(A2.8)}$$

  The energy of x is the value of the AF at the origin of the (ξ,τ) – plane, which corresponds to its maximun value:

  $$|A_x(\xi, \tau)| \leq A_x(0,0) = E_x, \forall \xi, \tau \quad \text{(A2.9)}$$

- Time-Frequency shift invariance:
  Shifting a signal in the time-frequency plane leaves its AF invariant apart from a phase factor (modulation):

$$y(t) = x(t - t_0)e^{j2\pi\nu_0 t} \Rightarrow A_y(\xi,\tau) = A_x(\xi,\tau)e^{j2\pi(\nu_0\tau - t_0\xi)} \qquad \text{(A2.10)}$$

- Interference geometry:
  In the case of a multi-component signal, the elements of the AF corresponding to the signal components are mainly located around the origin, whereas the elements corresponding to interferences between the signal components (AF-interference terms) appear at a distance from the origin which is proportional to the time-frequency distance between the involved components.

To illustrate the nature of the Ambiguity Function, the AF of the previous chirp signal is presented below. Fig. A2-5 shows how the Fourier transform maps the WVD auto-components to a region centered on the origin of the AF plane, whereas it maps the oscillatory WD cross-components away from the origin. In the below AF image, the AF auto-components corresponding to the three harmonics of the chirp lie superimposed at the center of the AF image, while the AF cross-components lie to either side. The components slant in the AF because the signal is chirping.

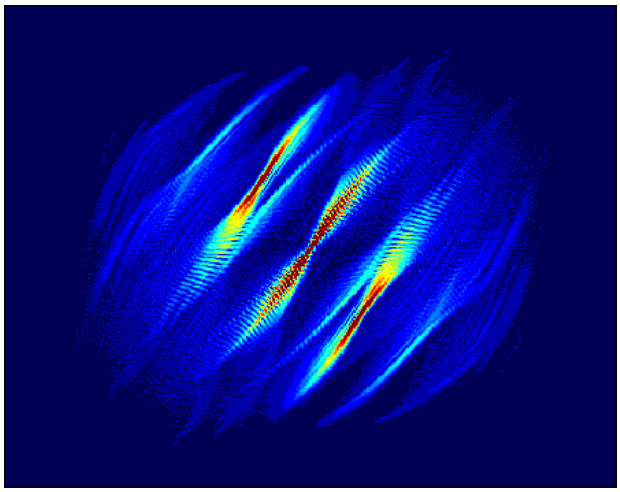

Figure A2-5. Ambiguity function of the bat chirp signal.
Delay runs horizontally and Doppler vertically, and the colors indicate energy level.

The Cohen's Class of TFRs

A great progress made by L. Cohen [A2.2], consisted of finding a general expression for all the energy time-frequency distributions which verified the property of time and frequency covariance. This property guarantees that, if the signal is Delayed in time and modulated, its time-frequency distribution is translated of the same quantities in the time-frequency plane. This class of distributions is called distributions of *Cohen's Class*, and its expression is the following:

$$C(t,f)_x = \iiint e^{j2\pi\xi(s-t)}\phi(\xi,\tau)x(s+\tau/2)x^*(s-\tau/2)e^{-j2\pi f\tau}\, d\xi ds d\tau \qquad \text{(A2.11)}$$

where $\phi(\xi,\tau)$ is a two-dimensional function called *parameterization function* or k*ernel*.

If we relate the Cohen's class with the ambiguity function, we can obtain a dual expression

$$C_x(t,f) = \int\int \phi(\xi,\tau)A_x(\xi,\tau)e^{-2\pi j(t\xi - f\tau)}d\xi d\tau \qquad \text{(A2.12)}$$

which is very instructive due to the role played by the kernel function. With this formulation, we can interpret the kernel as a masking function that tries to let the signal terms unchanged, and to suppress the interference cross-components. This masking operation defines a new TFR with different properties from the WVD.

Since there are many possible 2-d kernel functions, there exist many different TFRs for the same signal. The WVD is obviously a member of Cohen's class, with Kernel=1.

This characteristic presents a problem of kernel design optimization, since for any given signal, there are some TFRs which are better than others, in terms of extracting the more representative features. In order to show this variety of TFRs, two additional TFRs of the previous chirp signal are presented below: an almost optimal kernel TFR at left and the spectrogram at right (Fig A2-6).

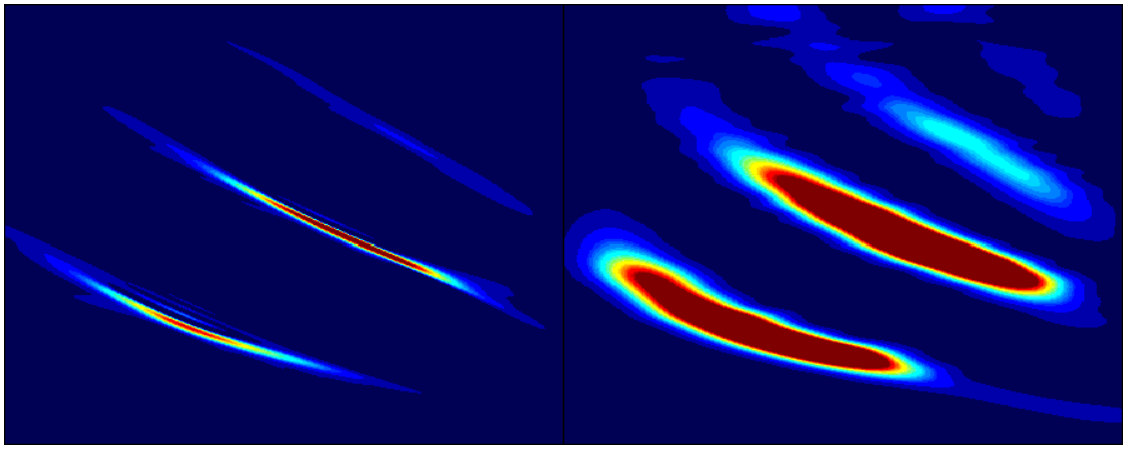

Figure A2-6. Kernel masked TFR and spectrogram of the bat chirp signal.
The spectrogram is the squared magnitude of the windowed short-time Fourier transform, and also belongs to Cohen's class. Its kernel is the AF of the short-time window function. Colors indicate energy level

The images of above come from the product of the Ambiguity Function with each respective kernel (Fig A2-7). The poor concentration of the spectrogram can be blamed

on the fact that the spectrogram kernel does not match the slanting AF auto-components of the chirp signal.

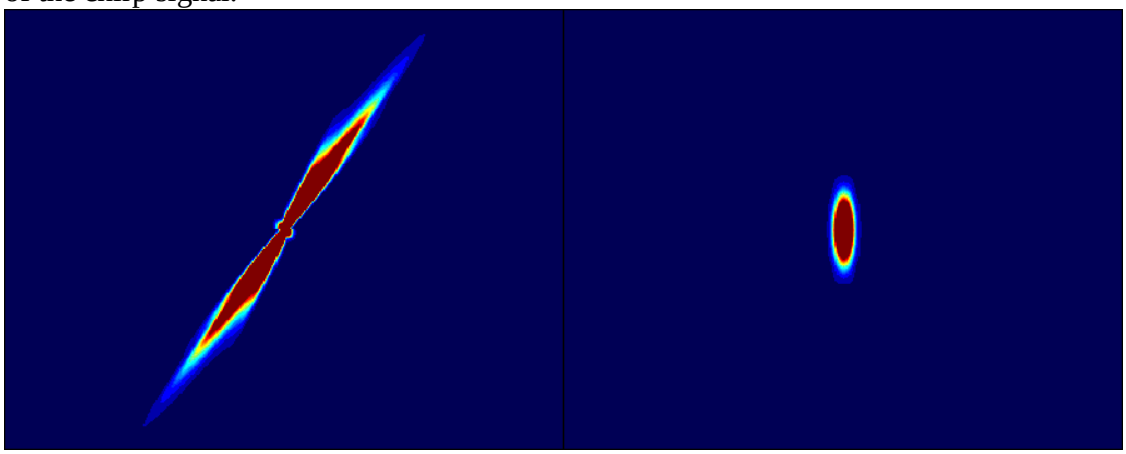

Figure A2-7. Kernel for the bat chirp signal at left and the spectrogram kernel at right.

Bibliography

Chapter 1

[1.1] K. L. Kilgore, P. H. Peckham, M. W. Keith, G. B. Thorpe, K. S. Wuolle, A. M. Bryden, and R. L. Hart, "*An implanted upper-extremity neuro-prothesis: Follow-up of five patients*," *J. Bone Joint Surg.*, vol. 79A, pp. 533–541, 1997.

Chapter 2

[2.1] E. R. Kandel, J. H. Schwartz, and T. M. Jessell, *Principles of Neural Science*, 3rd ed. New York: Elsevier/North-Holland, 1991.

[2.2] W. W. Orrison Jr., J. D. Lewine, J. A. Sanders, and M. F. Hartshorne, *Functions Brain Imaging*. St Louis: Mosby-Year Book, Inc, 1995.

[2.3] F. H. Lopes da Silva and A. van Rotterdam. *Biophysical aspects of EEG and MEG generation*. In E. Niedermeyer and F. H. Lopes da Silva, editors, *Electroencephalography*, pages 15-26. Urban & Schwarzenberg, München-Wien-Baltimore, 1982.

[2.4] George D Fuller, Ph.D. *BIOFEEDBACK Methods and Procedures in clinical practice* (1977).

[2.5] Blundell, G. G. *The meaning of EEG*. London: Audio Ltd.

[2.6] P.R. Kennedy and R.A.E. Bakay, "Restoration of neural output from a paralyzed patient by a direct brain connection", *NeuroRepor*t, v.9, pp. 1707- 1711, 1998.

[2.7] *The "10-20 System" of Electrode Placement.* http://faculty.washington.edu/chudler/1020.html

Chapter 3

[3.1] J.R. Wolpaw, D.J. McFarland, G.W. Neat, and C.A. Forneris. "*An EEG-based brain-computer interface for cursor control*". Electroenceph. Clin. Neurophysiol., v.78, pp. 252—258, 1991.

[3.2] G. Pfurtscheller, J. Kalcher, Ch. Neuper, D. Flotzinger, and M. Pregenzer, "*On-line EEG classification during externally-paced hand movements using a neural network-based classifier"*, Electroenceph. Clin. Neurophysiol.", v.99, pp. 416—425, 1996.

[3.3] J.M. Belsh and P.L. Schiffman (editors), *Amyotrophic lateral sclerosis: diagnosis and management for the clinicia*n, Futura Publishing Co., Inc., Armonk, NY, 1996.

[3.4] N. Birbaumer, N. Ghanayim, T. Hinterberger, I. Iversen, B. Kotchoubey, A. Kubler, J. Perelmouter, E. Taub, H. Flor. "*A Spelling Device for the Paralysed*". Nature, v.398, pp. 297—298, 1999.

[3.5] S. Lin, Y. Tsai, and C Liou, "*Conscious mental tasks and their EEG signals*", Medical and Biol. Engineering and Comput., v.31, pp. 421—425, 1993.

[3.6] *BRAIN-COMPUTER INTERFACES FOR COMMUNICATION AND CONTROL*, Gerwin Schalk, Dennis J. McFarland, and Jonathan R. Wolpaw, Laboratory of Nervous System Disorders, Wadsworth Center, New York State Department of Health and State University of New York at Albany: http://newton.bme.columbia.edu/wolpaw.html

[3.7] P.R. Kennedy and R.A.E. Bakay, "Direct control of a computer from the human central nervous system", *Brain-Computer Interface Technology: Theory and Practice: First International Meeting Program and Paper*s,The Rensselaerville Institute, Rensselaerville, New York, pp. 65—70, June 16-20, 1999.

[3.8] E.E. Sutter, "The brain response interface: communication through visually-induced electrical brain responses", *Journal of Microcomputer Application*s, v. 15, pp. 31—45, 1992.

[3.9] K.S. Jones, M.S. Middendorf, G. Calhoun, and G. McMillan, "Evaluation of an Electroencephalographic-based Control Device", *Proc. of the 42nd Annual Mtg of the Human Factors and Ergonomics Societ*y, pp. 491—495, 1998.

[3.10] M.S. Middendorf, G. McMillan, G. Calhoun, and K.S. Jones, "*Brain-computer interfaces based on the steady-state visual-evoked response*", Brain-Computer Interface Technology: Theory and Practice: First International Meeting Program and Papers, The Rensselaerville Institute, Rensselaerville, New York, pp. 78—82, June 16-20, 1999.

[3.11] T.M. Vaughan, J.R. Wolpaw, and E. Donchin, "EEG-Based Communication: Prospects and Problems", *IEEE Trans. on Rehabilitation Engineerin*g,4:4,pp. 425—430, 1996.

[3.12] R.M. Chapman and H.R. Bragdon, Evoked responses to numerical and non-numerical visual stimuli while problem solving, *Natur*e, v.203, pp. 1155 - 1157, 1964.

[3.13] S. Sutton and M. Braren and J. Zublin and E. John, Evoked potential correlates of stimulus uncertainty, *Scienc*e, v.150, pp. 1187 - 1188, 1965.

[3.14] Marco Onofrj, Donato Melchionda, Astrid Thomas, and Tommaso Fulgente, "Reappearance of event-related P3 potential in locked-in syndrome", *Cognitive Brain Researc*h, v.4, pp. 95 – 7 , 1996.

[3.15] L.A. Farwell and E. Donchin, “Talking off the top of the head: toward a mental prosthesis utilizing event-related brain potentials”, Electroenceph. Clin. Neurophysiol., pp. 510—523, 1988.

[3.16] F.H. Lopes da Silva, W.Storm van Leeuwen, and A. Remond, *Handbook of Electroencephalography and Clinical Neurophysiology: Volume 2, Clinical Applications of Computer Analysis of EEG and other Neurophysiological Signal*s, N. Elsevier Science Publishers}, Amsterdam, 1986.

[3.17] S. Devulapalli. "*Non-linear component analysis and classification of EEG during mental tasks*". Masters Thesis at Colorado State University, 1996.

[3.18] T. Fernandez, T. Harmony, M. Rodriguez, J. Bernal, and J. Silva. "*EEG activation patterns during the performance of tasks involving different components of mental calculation*". Electroenceph. Clin. Neurophysiol., v.94, pp. 175—182, 1995.

[3.19] B. Schneiderman. *Designing the user interface: Strategies for effective human-computer interaction*. 3 rd ed., Addison Wesley, Reading, Mass., 1998.

[3.20] G. Pfurtscheller, D. Flotzinger, and J. Kalcher, "*Brain-computer Interface – a new communication device for handicapped persons*", J. of MicrocomputerApplications, v.16, pp. 293—299, 1993.

[3.21] G. Pfurtscheller, D. Flotzinger, M. Pregenzer, J. Wolpaw, and D. McFarland. "*EEG-based Brain Computer Interface (BCI)*". Medical Progress through Technology, v.21, pp. 111-121, 1996.

[3.22] P.L. Nunez. *Neocortical Dynamics and Human EEG Rhythm*s. Oxford University Press, New York, 1995.

[3.23] J. Kalcher, D. Flotzinger, Ch. Neuper, S. Golly, and G. Pfurtscheller, “Graz brain-computer interface II: towards communication between humans and computers based on online classification of three different EEG patterns",*Medical and Biological Engineering and Computing*, v.34, pp. 382—388, 1996.

[3.24] D.J. McFarland, G.W. Neat, R.F. Read, and J.R. Wolpaw, "*An EEG-based method for graded cursor control*", Psychobiology, 21:1, pp. 77—81, 1993.

[3.25] P.R. Kennedy and R.A.E. Bakay, “Restoration of neural output from a paralyzed patient by a direct brain connection”, *NeuroRepor*t, v.9, pp. 1707— 1711, 1998.

[3.26] Bayliss, Jessica. *A Flexible Brain-Computer Interface.* Ph.D. Thesis, Computer Science Dept., U. Rochester, August 2001

Chapter 4

[4.1] Gupta, S.; Singh, H. *Preprocessing EEG signals for direct human-system interface*. Intelligence and Systems, 1996., IEEE International Joint Symposia on , 1996 Page(s): 32 –37.

[4.2] G. Gratton, M.G.H. Coles and E. Donchin. *A New Method for off – line removal of Ocular artifacts*. Electroencephalography and Neurophysiology, Vol 55, pp. 468-484, 1983.

[4.3] Nakamura A, Sugi T, Ikeda A, Kakigi R & Shibasaki H (1996). *Clinical application of automatic integrative interpretation of awake background EEG: quantitative interpretation, report making, and detection of artifacts and reduced vigilance level*. Electroencephalography and ClinIcal Neurophysiology 98:103-112.

[4.4] R. Bogacz, U. Markowska-Kaczmar, A. Kozik. *Blinking artefact recognition in EEG signal using artificial neural network.* In Proc. of 4th Conference on Neural Networks and Their Applications, Zakopane (Poland).

[4.5] Jung T-P, Makeig S, Westerfield W, Townsend J, Courchesne E, and Sejnowski TJ, "*Removal of eye activity artifacts from visual event-related potentials in normal and clinical subjects*" Clinical Neurophysiology, 111:10, 1745-58, 2000.

[4.6] B.W.Jervis, E.C.Ifeachor, and E.M.Allen. *The removal o ocular artifacts from the electroencephalogram :a review*. Medical &Biological Engineering &Computing , 26: 2-12, 1988.

[4.7] Vigario R, Sarela J, Jousmaki V, Hamalainen M, Oja E. *Independent component approach to the analysis of EEG and MEG recordings*. IEEE Trans Biomed Eng. 47(5): 589-93, 2000.

[4.8] Jung T-P, Humphries C, Lee T-W, Makeig S, McKeown MJ, Iragui V, Sejnowski TJ. *Removing electroencephalographic artifacts: comparison between ICA and PCA.* Neural Networks Signal Processing 1998b;VIII: 63–72.

[4.9] A. Schlögl and G. Pfurtscheller. *EOG and ECG minimization based on regression analysis*. Institute for Biomedical Engineering, Department of Medical Informatics, Univ. of Techn., Graz, Austria

Chapter 5

[5.1] I. Vincent. *Classification de Signaux Non-stationnaire*s. PhD thesis, Ecole Centrale de Nantes, 1995.

[5.2] P. Flandrin. *A time-frequency formulation of optimum detection.*" IEEE Trans. Acoust., Speech, Signal Processing, vol. 36, no. 9, pp. 1377-1384, 1988

[5.3] Atlas, L., J. Droppo, and J. McLaughlin, "*Optimizing Time-Frequency Distributions for Automatic Classification*". Proceedings of SPIE The International Society for Optical Engineering, Vol. 3162, San Diego, CA, pp. 161-171, July, 1997.

[5.4] D. Korosec. *Analysis of one-dimensional signals by processing of their time-Frequency representations*. Thèse de Doctorat, Université de Maribor, Université de Nantes (cotutelle), mai 1999.

[5.5] Duda, R. O. and Hart, P. E. 1973. *Pattern Classification and Scene Analysis*. Wiley, New York.

[5.6] M. Davy, "*Noyaux optimises pour la classification dans le plan temps-frequence*". PhD Thesis, Université de Nantes, septembre 2000.

[5.7] P. Leluc and R. Pantais. *Influence of Connexity in Signal Clasification*. Raport de stage de recherche de troisième année, Ecole Centrale de Nantes, 1999.

[5.8] R.G. Baraniuk and D.L. Jones. *A signal- dependant time-frequency representation : Optimal kernel design*. IEEE Transactions on Signal Processing, 41(4):1589–1601, 1993.

[5.9] H. Laurent and C. Doncarli. *"Stationarity index for abrupt changes detection in time-frequency plane"*. IEEE Signal processing letters, 5(2): 43-45, 1998.

[5.10] Jack Culpepper, *Discriminating Mental States Using EEG Represented by Power Spectral Density*, Department of Computer Science, Harvey Mudd College Claremont.

[5.11] E. Stolz. *Multivariate Autoregressive Models for Classification of Spontaneous Electroencephalogram During Mental Tasks*. Master's thesis, Electrical Engineering Department, Colorado State University, Fort Collins, CO, 1995.

Chapter 6

[6.1] Zachary A. Keirn. *Alternative modes of communication between man and machine*. Master's thesis, Purdue University, 1988.

[6.2] M. Osaka. *Peak alpha frequency of EEG during five mental tasks: lasks difficulty and hemispheric differences*. Psychophysiology, 21:101-105, 1984.

Annex 1

[A1.1] E. R. Kandel, J. H. Schwartz, and T. M. Jessell, *Principles of Neural Science*, 3rd ed. New York: Elsevier/North-Holland, 1991.

[A1.2] W. W. Orrison Jr., J. D. Lewine, J. A. Sanders, and M. F. Hartshorne, *Functions Brain Imaging*. St Louis: Mosby-Year Book, Inc, 1995.

[A1.3] F. H. Lopes da Silva and A. van Rotterdam. *Biophysical aspects of EEG and MEG generation*. In E. Niedermeyer and F. H. Lopes da Silva, editors, *Electroencephalography*, pages 15-26. Urban & Schwarzenberg, München-Wien-Baltimore, 1982.

Annex 2

[A2.1] François Auger, Patrick Flandrin, Olivier Lemoine, Paulo Gonçalvès. TIME-FREQUENCY TOOLBOX for Matlab.

[A2.2] Leon Cohen, *Time-Frequency Analysis*. Englewood Cliffs, NJ: Prentice-Hall, 1995.

[A2.3] Ming Li, Wei Zhao*, Weijia Jia. *The Profile of Kernels in Time Frequency Distributions*. Dept. of Computer Science, City University of Hong Kong, HK

[A2.4] Kozek, W.; Hlawatsch, F.; Kirchauer, H.; Trautwein, U. "*Correlative time-frequency analysis and classification of nonstationary random processes"*. Time-Frequency and Time-Scale Analysis, 1994., Proceedings of the IEEE-SP International Symposium on , 1994. Page(s): 417 –420